

PETROGRAPHIC CHARACTERIZATION OF TWO GOLD-RICH BANDED IRON FORMATIONS (BIFS) IN  
THE FOXE FOLT BELT  
BAFFIN ISLAND, CANADA

by

German Eduardo Gonzalez Garzon

A Prepublication Manuscript Submitted to the Faculty of the

DEPARTMENT OF GEOSCIENCES

In Partial Fulfillment of the Requirements

for the Degree of

PROFESSIONAL SCIENCE MASTER

In the Graduate College

THE UNIVERSITY OF ARIZONA

2010

**PETROGRAPHIC CHARACTERIZATION OF TWO GOLD-RICH BANDED IRON FORMATIONS (BIFs) IN THE FOXE FOLD  
BELT, BAFFIN ISLAND, CANADA**

Germán González Garzón

*Institute for Mineral Resources, Department of Geosciences, University of Arizona, and*

*AngloGold Ashanti Colombia S.A.*

**Abstract:**

Precambrian banded iron formations (BIFs) are an important host for gold mineralization in many cratons of the world, where they generally occur in greenstone belts and other supracrustal volcanic and/or sedimentary sequences of deep marine environments. The timing of gold mineralization relative to deposition of the BIFs (i.e., syngenetic versus epigenetic) commonly is controversial, yet the two interpretations imply contrasting exploration techniques to be effective. Two gold prospects have been studied, from several that have been identified in BIFs within the Bravo Lake Formation in the Early Proterozoic Pilling Group, which form part of the Foxe Fold Belt, in central Baffin Island, Canada. Petrographic characterization and microprobe analysis of 56 samples from the Bravo Lake Formation have defined at least two metamorphic events and sulfidation states for gold deposition and related mineralization. These results show a close textural association of gold and loellingite ( $\text{FeAs}_2$ ), which implies that arsenic should be a good pathfinder element for regional gold exploration. However, conclusive evidence for epigenetic or syngenetic origin of gold deposition in this region is still elusive, in part because of the intensity of deformation and grade of metamorphism, and both options have to be considered in order to do exploration for new prospects on Baffin Island. Comparisons between these two projects and deposits of gold-bearing BIF worldwide are very important in order to indicate potential future work and analyses to be done on Baffin Island.

## Introduction

Banded iron formations (BIFs), first defined by James (1954), are thinly-bedded or laminated chemical sediment, with anomalously high iron content, generally interbedded with chert. BIFs are divided into four categories based on bulk composition, namely oxide-, carbonate-, silicate-, and sulfide-rich iron formation. There is general agreement on the origin of oxide-, carbonate-, and silicate-rich facies, as corresponding to marine chemical and/or diagenetic sediment (Castro, 1994; Klein and Ladeira, 2000; Klein, 2005), but the origin of sulfide-rich BIFs is still a matter of controversy. Gold is almost exclusively related with this facies of BIFs; therefore, if gold is syngenetic (Ridler, 1970; Hutchinson et al., 1971; Hutchinson, 1976; Fripp, 1976; Saager et al., 1987; Slack et al., 2007) with the sediments, exploration has to be directed by stratigraphic constraints; on the other hand, if the gold is epigenetic (Fyon et al., 1983; Phillips et al., 1984; Bullis et al. 1993), structures and conduits become relevant for exploration purposes.

Worldwide gold production and reserves in BIFs exceeds 3000 tonnes (Kerswill, 1995). Some of the biggest gold-bearing BIF deposits are Homestake, South Dakota, USA; Morro Velho and Cuiaba, Brazil; Lupin, Northwest Territories, Canada; and Vubachikwe, Zimbabwe.

Henderson et al. (1989), Corrigan et al. (2001), and Scott et al. (2003) compiled and contributed to the general geology of central Baffin Island, and Stacey and Pattison (2003) and Stacey (2005) provided more detail regarding the stratigraphy of the Bravo Lake Formation, which occurs within the Piling Group (Fig. 1). The Piling Group is a sequence of Lower Proterozoic (ca. 1.9 Ga, Wodicka et al., 2002) supracrustal rocks that form part of the Foxe Fold Belt in central Baffin Island. The Bravo Lake Formation of the Piling Group is host to two gold prospects, namely Malrok and Ridge Lake (Fig. 2). The Bravo Lake Formation comprises mafic volcanic rocks interlayered with siliciclastic and minor chemical sedimentary rocks and BIFs, all intruded by mafic and ultramafic sills. These rocks were complexly deformed by thrusting, at least three phases of folding, and upper amphibolite and lower granulite facies of metamorphism.

Petrographic descriptions and microprobe analyses were performed on 56 polished thin sections of BIFs and wall rocks of the Bravo Lake Formation to characterize mineralogically the BIF-hosted gold orebodies and to understand local controls on mineralization. The evidence presented will demonstrate that hydrothermal alteration associated with gold mineralization is absent, though

retrograde metamorphic minerals are present but the absence of alkali metasomatism in BIFs is due to insufficient aluminum to stabilize any potassium-bearing phases (Goldfarb, 2005). Petrographic observations also show a close textural relationship between gold, occurring as inclusions, in loellingite ( $\text{FeAs}_2$ ), although compelling evidence for the mechanism of gold deposition was not observed. Pyrrhotite is the most abundant sulfide, usually with inclusions of chalcopyrite, and seems to be deposited subsequent to gold. Pyrrhotitization occurs apparently at the expense of preexisting pyrite, magnetite, and ilmenite. On the other hand, some mineralization crosscuts stratification and also occasionally fills fractures in garnets. This observation provides evidence that some remobilization of sulfides, if not most mineralization, occurred post peak-metamorphism. At least two superimposed metamorphic events of upper amphibolite facies were identified, with some assemblages transitional to granulite facies (Fig. 3).

### **Banded Iron Formations**

Banded iron formation (BIF) is defined as a finely bedded or laminated sedimentary rock with anomalously high iron content (James, 1954) and sometimes, but not always, interbedded with chert; even when they are metamorphosed, the relict banding is usually still evident. BIFs commonly occur in greenstone belts and other Precambrian supracrustal sequences, and their age are restricted from ca. 3.8 Ga to ca. 1.8 Ga, although there are a few, atypical BIFs that formed between 0.8 to 0.6 Ga (Klein, 2005). BIFs occur usually in sedimentary and volcanic sequences with deep-sea floor affinity, and most of these sequences have suffered different degrees of metamorphism, typically low to medium grade (i.e., greenschist and lower amphibolite facies, Gole and Klein, 1981; Hodgson and MacGeehan, 1982; Martins et al., 2007). James (1954) divided BIFs into four main facies, depending on the dominant mineralogy: oxide-, carbonate-, silicate-, and sulfide-rich facies.

There is agreement on the origin of oxide-, carbonate-, and silicate-rich facies of BIFs, corresponding to marine chemical and/or diagenetic sediment (Castro, 1994; Klein and Ladeira, 2000; Klein, 2005), possibly by hydrothermal vents or plumes (Slack and Cannon 2009) or exhalative volcanogenic source (Saager et al., 1987) in a stratified water column under anoxic conditions, without detrital input. On the other hand, the origin of sulfide-rich BIFs has been extensively debate among authors supporting an epigenetic or a syngenetic origin. Gold mineralization is strongly related to sulfides in these deposits (Fripp, 1976; Phillips et al., 1984),

mainly arsenopyrite. The genesis of gold and sulfides have major implications on exploration philosophy; as discussed below.

The criteria for syngeneses (Ridler, 1970; Hutchinson et al., 1971; Hutchinson, 1976; Fripp, 1976; Saager et al., 1987) are the close spatial relation between BIFs and volcanogenic sequences; the stratiform character of the deposits and their lateral persistence; the narrow layers and their rhythmical banding among the BIFs; and in some cases the absence of a feeder zone (Nelson, 1985) or wall-rock alteration. For targeting ore with that has a syngenetic origin, exploration should be focused on stratigraphic controls and variations, bearing in mind structural complications, but not structures as mineralization traps.

On the other hand, the criteria for epigenesis are the lateral transition between sulfide-rich plus gold layers and sulfide-free oxide- or carbonate-rich BIF (Fyon et al., 1983; Bullis et al. 1993); zonation of the alteration surrounding mineralization zones (Martins et al., 2007); strong structural control on mineralization (Phillips et al., 1984; Ribeiro et al., 2007); the absence of sulfide-rich facies (though minor pyrite is usually present) within the least metamorphosed and well-preserved BIF (Klein, 2005); textures indicating replacement of iron oxides by iron sulfides (Vielreicher et al., 1994); and absence of mineralization within the primary sedimentary environment. Further geochemical and mineralogical evidence is given by Wyman et al. (1986) and Salier et al. (2005) and mass balance calculations of Groves et al. (1988) argue against lateral movement of background gold from barren to mineralized BIFs. The bulk chemistry shown by Klein (2005) for BIF worldwide present a markedly difference with sedimentary rocks associated with volcanic-hosted base metal deposits, particularly because the former have extremely low contents of sulfur and also lower amounts of  $Al_2O_3$  than the latter. For targeting ore that has an epigenetic origin, exploration is focused primarily on structures that may control movement and deposition of metals, for example, faults, discontinuities, shear zones, or fold hinges.

Considering an epigenetic origin, another point of discussion is the source of the fluids responsible of mineralization. The proximity of gold-rich BIF with granitoids and intrusive centers have suggested a magmatic source for these fluids (e.g., Superior Craton, Valliant and Hutchinson, 1982; Wyman et al., 1986; Colvine, 1988); however, there are gold deposits far from any intrusive rocks (e.g., Quadrilatero Ferrifero, Martins et al., 2007). There has been further geochemical and geochronological evidence for a distal and deep source for such deposits (Salier et al., 2005), and

some authors have argued in favor of metamorphic origin for the ore fluids (Groves et al., 1982; Martins, 1995 in Martins et al., 2007). Gold-rich fluids may have flowed through structures and been deposited with sulfides in Fe<sup>2+</sup>-rich BIFs. Oxidation of sulfur is the mechanism capable of reducing Au<sup>1+</sup> and precipitating as Au<sup>0</sup>. Gold and sulfur show a positive correlation, evidence that they should have been deposited synchronously (Phillips et al., 1984).

### **Geologic Setting**

The Foxe Fold Belt (Fig. 1) is located in central Baffin Island, and it extends onto the Melville Peninsula, where it is correlated with the Rinkian Belt in western Greenland (Taylor, 1982; Hoffman, 1988). The main stratigraphic unit is the Pilling Group (Fig. 2), which was deposited unconformably over the Archean Rae Province, its northern limit, and flanked to the south by the ca. 1.85 Ga Cumberland Batholith (Corrigan et al., 2001; Wodicka et al, 2002 ;Scott et al., 2003).

#### *Stratigraphy*

*Rae Craton:* The Archean Rae Craton contains rock with ages of between 2.70 and 2.85 Ga (Wodicka et al., 2002), and it is composed mainly of banded granodiorite to monzogranitic orthogneiss, several micmatitic granitoid plutons, and minor migmatitic siliciclastic and volcanic rocks (Scott et al., 2003).

*Pilling Group:* The Pilling Group is the major tectono-stratigraphic unit of the Foxe Fold Bent in Baffin Island (Stacey and Pattison, 2003), and it is divided into five units, namely, Dewar Lakes Formation, Flint Lake Formation, Bravo Lake Formation, Astarte Formation, and the massive Longstaff Bluff Formation; the thicknesses of all units varies considerably, in part for differences in depositional environment but also because of tectonic complexity. The age of the whole group is constrained by detrital zircon ages of the lowermost unit, ca. 2.17 Ga, and by a diorite sill within the Bravo Lake Formation with U-Pb zircon age of ca. 1883 Ma. Longstaff Bluff Formation is thought to be younger than this last age because it overlain by the Bravo Lake Formation.

*Dewar Lakes Formation:* The Dewar Lakes Formation unconformably overlies the Rae Craton and is the lowest stratigraphic unit of the Pilling Group. It includes quartzite and feldspathic quartzite with minor beds of muscovite schist (Corrigan et al., 2001; Scott et al., 2003). Locally, the quartzite can contain sillimanite.

*Flint Lake Formation:* Overlain the quartzites of the Dewar Lakes Formation, are dolostone, marble, and calc-silicate units of the Flint Lake Formation (Corrigan et al., 2001;). Minor amounts of siliciclastic beds are also present. This unit is interpreted to represent the same stratigraphic position of the Bravo Lake Formation because both units overlie the Dewar Lakes Formation and both are overlain by the graphitic pelites of the Astarte River Formation (Scott et al., 2003).

*Bravo Lake Formation:* The Bravo Lake Formation overlies the metasedimentary rocks of the Dewar Lakes Formation and is composed of mafic volcanic rocks interbedded with minor sedimentary rocks. The Bravo Lake Formation also contains mafic and ultramafic sills. Several segmentary rocks within Bravo Lake Formation are interpreted as silicate- and sulfide-rich BIFs. The thickness of this unit may vary from less than 100 m up to several hundreds of meters. Stacey and Pattison (2003) and Stacey (2005) subdivided this formation in five units around the Malrok prospect area.

Unit 1: Mafic flows and mafic and ultramafic sills characterize the base of the Bravo Lake Formation with minor amounts of metasedimentary rocks. These psammities and pelites are accompanied by silicate-rich BIF finely interbedded with chert (quartzite). A high percentage of sulfides appears to be disseminated in the BIF layers. Gold-rich zones have been identified within the BIF of this unit in the Ridge Lake area, and probably in the Malrok area as well. The characteristics of this mineralization will be described and discussed below.

Unit 2: This unit is characterized by a metamorphosed sequence of pillow basalts up to 200 m. The minerals present are plagioclase and clinopyroxene in a matrix of amphibole and plagioclase.

Unit 3: Up to 300 m of metasedimentary rocks with amphibole, biotite, garnet, and quartz overlie the pillow basalts; minor quartzites, ultramafic sills, and silicate- and sulfide-rich BIFs are also present. Gold-rich BIFs belonging to this unit are present in both Ridge Lake and Malrok areas. These BIFs have pyroxene, amphibole, garnet, biotite, and quartz, and the most abundant sulfide is pyrrhotite.

Unit 4: The unit 4 is characteristically composed of massive metavolcanic rocks up to 300 m thick. The mineralogy is characterized by porphyroblasts of clinopyroxenes in a matrix of finer grained amphiboles. These metavolcanic rocks are interbedded with minor metasedimentary layers of similar mineralogy.

Unit 5: The last unit of Bravo Lake Formation is at least 75 m thick and is composed of psammite and sulfide-rich siliciclastic rocks and silicate- and sulfide-rich BIF, rarely intruded by ultramafic sills, which are more abundant in the middle part of this unit.

**Banded Iron Formations (BIFs):** Several gold prospects have been identified within the Bravo Lake Formation by Commander Resources Ltd., but only two of them are studied here. These two, namely the Malrok and Ridge Lake prospects, are the better sampled and drilled than other prospects. These two prospects are located on the western margin of central Baffin Island, some 50 km from Wordie Bay, which is on the west coast of Baffin Island (Fig. 2). The prospects consist mainly of silicate- and sulfide-rich BIFs that are continuous for several kilometers. The mineralogy and mineralization of these BIFs will be discussed in detail below.

**Astarte Formation:** This unit overlies in different places the three formations described above, and the Astarte Formation consists of graphitic pelite and semipelite, black shales, and sulfide-rich BIF (Corrigan et al., 2001; Scott et al., 2003). Biotite, muscovite, and sillimanite appear in this unit, depending on the predominant metamorphic grade.

**Longstaff Bluff Formation:** This is the topmost unit of the Pilling Group and comprises thin- to thick-bedded psammite and feldspathic wacke, with thin intercalations of semipelite (Corrigan et al., 2001; Scott et al., 2003). Calc-silicate pods up to several tens of centimeters, after carbonate concretions, appear within the psammitic beds. These metaturbidites occupy a large area of the central Baffin Island. This is the thickest formation in the Pilling Group, probably up to a few kilometers thick.

**Cumberland Batholith:** The most prominent intrusive body that intrudes the Pilling Group to the south is the Cumberland Batholith, with an age of ca. 1.85 Ga. Some smaller intrusive bodies also can be correlated with this batholith and have similar ages (Corrigan et al., 2001; Wodicka et al., 2002). These batholiths are granodioritic and monzogranitic in composition, and the rocks have K-feldspar megacrysts, biotite, and minor hornblende. These plutons are intruded by younger monzogranite dikes and plutons with garnet, biotite, and minor muscovite and cordierite. This magmatism is interpreted as partial or total melting of the Longstaff Bluff Formation, the last meta-turbiditic unit of the Pilling Group.

Undeformed and unmetamorphosed diabase dikes, nearly vertical, are widespread in the whole area and vary from several meters to hundreds of meters in width. These dikes have an age of ca. 723 Ma (Scott et al., 2003) and can be traced for several tens of kilometers.

#### *Structural Setting and Metamorphism*

Three phases of Early Proterozoic deformation ( $D_1$ ,  $D_2$ ,  $D_3$ ) have been interpreted by several authors in the area (Henderson et al., 1989; Corrigan et al., 2001; Wodicka et al., 2002). The first phase ( $D_1$ ) corresponds with a thin-skinned deformational event that produces several low-angle repetitions that regionally produced a northwest-trending mineral lineation interpreted to be contemporaneous with the first regional peak metamorphic event ( $M_1$ ).  $D_1$  is also responsible for the overthrusting of the Bravo Lake Formation onto the Longstaff Bluff Formation and for the emplacement of the Cumberland Batholith. The  $M_1$  metamorphic event reaches granulite facies and migmatitic conditions.

Deformational events  $D_2$  and  $D_3$  are described as thick-skinned deformational events as they involve Archean basement.  $D_2$  produced northeast-trending folds, and  $D_3$  produced north-trending folds. The intersections of the two sets of folds produced the characteristic dome-and-basin geometry of the Pilling Group in the area. U-Pb dates of Bethune and Scammell (2003) suggest that  $D_2$  occurred at 1.83-1.82 Ga, whereas Wodicka et al. (2002) interpret an age of 1.80 Ga for  $D_3$  folding.  $M_2$  is coeval with  $D_2$  and varies in grade from lower amphibolite to migmatitic conditions. Folding of  $D_2$  migmatites and recrystallization at low temperature correspond with  $D_3$  deformational event. The  $D_3$  deformation event also is characterized by several retrograde minerals such as andalusite, muscovite, chlorite, and green biotite at the expense of  $D_2$  minerals (Henderson et al., 1989).

#### **Ownership of the Project**

Commander Resources Ltd. is the current owner of Baffin Island Gold Project, which includes the two studied prospects, Malrok and Ridge Lake. Several holes have been drilled there, but it is not yet possible to estimate ore reserves or mineral resources. Commander Resources Ltd. is the operator of the project, but work is funded by AngloGold Ashanti under the terms of a \$20-million and six year Farm-in JV Agreement announced on September 3, 2009. At the end of those six years, AngloGold Ashanti will become the owner of 51 percent of the property, and will be able to

increase its ownership to 70 percent by funding all expenditures through the completion of a feasibility study. The agreement can be seen in the web page of Commander Resources Ltd.

## **Analytical Methods**

### *Petrography*

Transmitted and reflective light microscopy studies were done on 56 polished thin sections from Malrok and Ridge Lake prospects. All samples are from drill core and include gold-bearing BIFs, upper and lower barren wall-rocks, and one quartz vein. Results of this work include textural and mineralogical descriptions, assessment of the metamorphic grade, and description of mineralization. Selected photomicrographs illustrate the descriptions.

### *Microprobe*

From the 56 polished thin sections, 15 representative samples were selected for four different microprobe analyses on a CAMECA SX50 microprobe. High-quality Wavelength Dispersive Spectrometry (WDS) analyses of several minerals provided accurate, non-destructive, quantitative chemical analyses (Tables 1, 2, and 3) to characterize the compositions of several minerals. Rapid Energy Dispersive Spectrometry (EDS) analyses permitted chemical identification of several unknown minerals. X-ray maps of seven thin sections were done to image the spatial distribution of some elements (e.g., gold) within these samples. These techniques provided chemical and textural evidence for the association of gold with other elements. Finally, faster and smaller X-ray maps were made to describe the chemical zoning within a single mineral and to document the chemical association of gold.

## **Mineralogy**

### *Silicates and gangue minerals*

*Quartz:* This is the most ubiquitous mineral in all assemblages, although proportion and size are highly variable. Lower proportions were observed in high grade rocks in Malrok zone, whereas in some samples from Ridge Lake, where metamorphic grade is lower, quartz is a major constituent (e.g., Fig. 4). Most times this mineral is present in mosaics with triple junctions between grains with variable sizes, as mentioned before. Sometimes differences in sizes or in proportions relative

to other minerals represent the distinction between micro and mesobands whereas other times, this differentiation is marked by the presence or absence of this mineral. This lamination may represent syndimentary structures, though quartz is now recrystallized.

*Biotite*: The variety annite is the biotite present in biotitic schists, more abundant in Ridge Lake project where metamorphic grade is lower (Fig. 5). Most times single euhedral crystals are lined with foliation. Retrograde biotite are sometimes present in mafic granulites in Malrok and green biotites, where present with brown biotites, are also interpreted as retrograde in Ridge Lake schists. A typical chemical formula for biotites observed in this work would be  $K(Fe_{0.6},Mg_{0.3},Al_{0.1})_3Al_{1.3},Si_{2.7}O_{10}(OH)_2$ .

*Orthopyroxene*: This mineral occurs only at Malrok project as coarse and generally anhedral grains; sometimes they have inclusions of amphiboles and/or pyrrhotite. They do not show any evidence of instability with grunerite, which means that both grow in equilibrium as prograde minerals until peak-metamorphism; the same is true for clinopyroxenes (Fig. 6). Their composition plots in the field of ferrosilite (Fig. 7) with amount of Ca, Mg, and Mn ranging in 0.38-0.71, 2.0-2.4, and 4.2-4.8 weight percent respectively. The association of this mineral with clinopyroxene and grunerite are typical of the transition between upper amphibolite and lower granulite facies; however, when olivine is present, these indicate the transition to upper granulite facies, a very high temperature metamorphic grade (Fig. 3). Chemical formula of ferrosilite in these samples is  $(Fe_{0.8},Mg_{0.1},Mn_{0.1})_2Si_2O_6$ .

*Clinopyroxene*: Textural characteristics of both, orthopyroxene and clinopyroxene are very similar. However, only clinopyroxene is present in Ridge Lake, where it has inclusions of quartz, grunerite, and/or ferro-actinolite. Very fine exsolution lamellae were identified in the microprobe, but the size of those were under the detection limit of the beam so it is unknown their difference in composition, probably different proportions of calcium. Composition of clinopyroxenes is more variable than orthopyroxene, plotting mostly in the field of hedenbergite and only one after in the diopside field (Fig. 7), but near the limit with hedenbergite. Typical formula of hedenbergite could be  $(Ca_{0.9},Fe_{0.7},Mg_{0.3},Mn_{0.1})Si_2O_6$ .

*Amphibole*: Data reduction (Table 1) for these minerals followed procedures of Schumacher (1997) appendix in Leake et al. (1997). Three types of amphiboles were identified (Figs. 8 and 9), with

distinctive textural characteristics. Grunerite (with the formula  $[(\text{Fe}_{0.7}, \text{Mg}_{0.2}, \text{Mn}_{0.1})_7 \text{Si}_{8.0} \text{O}_{22} (\text{OH})_2]$ ) is the most ubiquitous amphibole and is present in almost all assemblages. Grunerite may form, probably with some ferro-actinolite, up to 80 modal percent of some BIF samples. Typically it forms fan aggregates, although lineated single grains are also very common. In some cases smaller grunerite grains are included in garnet and/or pyroxenes. This amphibole is the mineral most frequently, but incipiently altered to serpentine.

Ferro-actinolite (with the formula  $\text{Ca}_{1.9}(\text{Fe}_{0.4}, \text{Mg}_{0.5}, \text{Mn}_{0.1})_5 \text{Si}_{8.0} \text{O}_{22} (\text{OH})_2$ ) is frequently found as single and fine grained acicular grains, most commonly with green pleochroism, associated with quartz bands or as euhedral aggregates forming bands. Ferro-actinolite is restricted to Ridge Lake samples, where the metamorphic grade is lower.

Finally, calcian ferro-gedrite (with the formula  $[(\text{Fe}_{0.2}, \text{Mn}_{0.6}, \text{Ca}_{0.2})_5 (\text{Al}_{0.7} \text{Fe}_{0.3})_2 \text{Si}_{5.7} \text{Al}_{2.3} \text{O}_{22} (\text{OH})_2]$ ) was identified in some samples from the Malrok zone; it forms anhedral and very fine grains, mainly as a retrograde mineral, in some bands constituting aggregates with other retrograde minerals such as chlorite and calcite, probably as alteration products of grunerite and/or almandine.

*Garnet:* Garnets are present in both projects and related with almost all lithologies in different proportions, up to 30 volume percent in some samples. All garnets are almost almandine in composition with low spessartine and grossular components (Table 3). They appear as subhedral to euhedral porphyroblasts (Fig. 5), sometimes with poikilitic texture, and sometimes exhibiting syn-deformational rotation. Frequently, some garnets contain inclusions of quartz, amphibole, graphite, and/or ilmenite (Fig. 10). A typical chemical formula for these garnets is  $(\text{Fe}_{0.7}, \text{Mn}_{0.1}, \text{Ca}_{0.1}, \text{Mg}_{0.1})_3 \text{Al}_2 (\text{SiO}_4)_3$ , and is the major aluminum-bearing mineral phase in the studied samples (Fig. 11).

*Olivine:* Fayalite was identified only in one sample from Malrok zone as coarse anhedral grains with characteristic high relief and slightly yellowish pleochroism. This mineral is representative of the highest metamorphic grade described among all samples: upper granulite facies. Chemical formula for this fayalite is  $(\text{Fe}_{0.8}, \text{Mg}_{0.2}, \text{Mn}_{0.2})_2 \text{SiO}_4$ .

*Carbonate:* Occurrences of carbonates are few, and most of the time carbonate occurs in trace amounts. WDS analyses of prograde carbonates show ankeritic compositions, whereas retrograde carbonates, which are mostly filling fractures and altering amphiboles, are mainly calcite.

*Plagioclase:* A few crystals of andesine were identified in only one sample, as fine anhedral grains associated with quartz in the Ridge Lake zone. The chemical formula of the plagioclase identified is  $(\text{Na}_{0.66}, \text{Ca}_{0.34})(\text{Si}_{2.6}, \text{Al}_{1.4})_4\text{O}_8$ .

*Stilpnomelane:* Prograde stilpnomelane appears as acicular radial aggregates in very few samples from Ridge Lake zone (Fig. 4), associated with quartz-amphibole schists. Rocks with stilpnomelane may represent the lowest metamorphic grade in the studied rocks, probably upper greenschist or lower amphibolite facies. Another type of stilpnomelane (green and brown, not acicular) of this mineral is mainly filling rock and mineral fractures and also incipiently altering amphiboles and pyroxenes. Therefore, it is interpreted as a retrograde occurrence, consistent with its association with other retrograde minerals such as chlorite. Normalization of microprobe analyses for this mineral is particularly difficult because of its high content of water; hence, it is also possible that the retrograde type of stilpnomelane can be serpentine, because it has very low potassium content, less than 0.04 wt percent, in the retrograde occurrences.

*Chlorite:* The pennine variety of chlorite is a fairly common retrograde mineral, occurring as alteration of amphiboles, though always in small amounts. Chlorite is associated with other retrograde minerals such as calcite and/or epidote.

*Epidote:* Local epidote was observed in only a few samples as very fine grains associated with calcite and chlorite, usually as alteration products of garnets or amphiboles.

*Talc:* This mineral was found only in very small amounts, as a very incipient alteration product in certain amphiboles.

*Graphite:* This is an abundant mineral in biotitic schists, but graphite is also present in small proportions in other lithologies.

Apatite, xenotime, zircon, and allanite or francoisite (Ce-Sm-Nd-bearing mineral) were identified in some samples using the EDS technique, but they represent very rare phases in these rocks.

#### *Sulfides, oxides, and other metals*

*Pyrrhotite:* This is the most abundant and ubiquitous sulfide in the studied samples; proportions are up to 50 modal percent in a few thin sections. It is present as mosaics in bands and/or

disseminated, and sometimes crosscut the metamorphic fabric and/or garnet crystals (Fig. 12). Pyrrhotite is strongly associated with garnet-rich bands but also is present with pyroxenes, amphiboles, and biotite. In some samples, it replaces pyrite, magnetite, and/or ilmenite (Figs. 13 and 14). Pyrrhotite always has inclusions of chalcopyrite in different proportions, and sometimes single euhedral arsenopyrite grains are surrounded by pyrrhotite. The chemical formula found in several analyses was  $\text{Fe}_{0.93}\text{S}_{1.07}$ .

*Pyrite:* Very few pyrite grains were observed, occurring as relict grains replaced by pyrrhotite grains (Fig. 13), but also probably altering pyrrhotite along fractures. A microprobe analysis gives a common chemical formula,  $\text{FeS}_2$ .

*Loellingite:* This mineral appears always as irregular relicts coring euhedral to subhedral arsenopyrite grains. Up to 5.5 and 2.1 weight percent of nickel and cobalt (Figs. 15 and 16) were identified, respectively, with the WDS technique within the mineral structure of loellingite. Some loellingite grains contain gold, bismuth, and maldonite as inclusions, although more than 30 percent of the total gold grains (Table 4) precipitated at in the boundaries between loellingite and arsenopyrite (Figs. 17 to 22). These inclusions have sizes up to 95  $\mu\text{m}$  in diameter and are irregular in shape. The chemical formula is close to  $(\text{Fe}_{0.76}, \text{Ni}_{0.19}, \text{Co}_{0.08})\text{As}_{1.93}$ .

*Arsenopyrite:* This mineral is present as euhedral to subhedral grains up to 4 mm in diameter, usually surrounded by massive mosaics of pyrrhotite. Some grains are cored by irregular relicts of loellingite, which is where most of the gold is present (Figs. 17 to 22). The chemical formula obtained with WSD analyses was  $\text{Fe}_{1.2}\text{As}_{1.1}\text{S}_{0.97}$ .

*Magnetite:* This oxide mineral is more abundant in the Malrok zone, where it is present frequently in relative small amounts up to a 2 modal percent. In these rocks, magnetite is being replaced by pyrrhotite (Figs. 13 and 14). Analyses gave a very typical formula:  $\text{Fe}^{+2}\text{Fe}^{+3}_2\text{O}_4$ .

*Ilmenite:* This mineral is abundant as euhedral and lineated grains in some samples from the Ridge Lake zone in biotitic schists, which also contain biotite, graphite, and garnet (Fig. 10). In some samples, similar to magnetite, it seems to be partially replaced by pyrrhotite. A representative formula obtained was  $\text{Fe}_{0.95}\text{Ti}_{1.1}\text{O}_3$ .

*Chalcopyrite:* This is another ubiquitous mineral (Fig. 12), but it occurs in minor amounts and mostly as inclusions within pyrrhotite. Microprobe analyses gave  $\text{Cu}_{0.98}\text{Fe}_{1.2}\text{S}_2$  as the chemical formula.

*Sphalerite:* Single grains commonly appear in trace amounts where sulfides are abundant, mostly associated with pyrrhotite (Fig. 12).

*Native bismuth and maldonite:* Both minerals were analyzed with WDS technique and are closely associated with deposition of gold within, and at the borders with, relicts of loellingite (Fig. 22). The chemical formula obtained for maldonite was  $\text{Au}_2\text{Bi}_{0.99}$ .

#### *Gold: occurrence and mineralogical characteristics*

Gold is closely associated with loellingite, where it is present as irregular inclusions accompanied by bismuth and/or maldonite (Figs. 17 to 22). Almost 60 percent of gold grains are as inclusions in loellingite; 15 percent as inclusions arsenopyrite; 7 percent as free gold associated with quartz; and less than 15 percent associated with other silicates such as pyroxene, amphibole, or garnet (Fig. 14). Diameters of single gold grains vary from 1 to 95  $\mu\text{m}$ , averaging 9.4  $\mu\text{m}$ . Detailed data on gold occurrence and mineral association are tabulated in Table 4. The fineness of gold analyzed in the microprobe varies from 719 to 998, and impurities include silver, arsenic, bismuth, and sulfur. The gold/silver ratio measured with WDS varies from 4.2 to 44.1; lower ratios were found in gold inclusions in loellingite whereas higher ratios correspond with free gold associated with a pyroxene. These two characteristic and dissimilar ratios could imply the presence of two different gold sources, one related with the first mineralization event and another one, with higher ratios, probably syn- or post-second mineralization event; however, data are too limited to draw firm conclusions.

#### *Schists*

Biotite + quartz + garnet  $\pm$  graphite schists are common rock types in the Ridge Lake zone in both, BIFs and wall-rocks. They have variable but low amounts of amphiboles, clinopyroxenes, and ilmenite, whereas pyrrhotite contents can be considerable where they are mineralized. Foliation is parallel to its well-preserved banding, which varies in thickness from 1 to 10 mm.

#### *Amphibolitic Gneisses*

Amphibolic and minor clinopyroxenic gneisses are presented in Ridge Lake and have variable amounts of garnet and quartz. Amphibole proportions locally are up to 80 modal percent of a thin section. Sulfides can be abundant, generally restricted to specific bands where garnet is also present. This kind of rock can be present in BIFs and in wall rocks. Bedding is also preserved, but it is more irregular and foliation is parallel to it.

#### *Granulites and Pyroxenic Gneisses*

Massive and banded granulites are characterized by ortho- and clinopyroxenes with minor proportions of amphiboles, quartz, garnet, ankerite, and in only one sample, fayalite. Foliation is not always evident in thin section but is common. Granulites are restricted to the Malrok zone and are present in both BIFs and wall rocks.

#### *Quartzites*

Quartz content can be high in some samples and quartz veins are reported in the Ridge Lake zone. Minor amounts of amphibole, biotite, and garnet are present, and they locally can have sulfides content up to 20 percent. Quartzites are present in BIFs and wall rocks and are commonly interbedded with schist or sulfide-rich BIF.

## **Discussion**

#### *Metamorphism*

At least two metamorphic events ( $M_1$  and  $M_2$ ) were identified in the Ridge Lake zone, where differences in zonation and inclusions in garnet porphyroblasts (Fig. 5) characterized each event; this is in agreement with observations made by Scott et al. (2003) and Henderson et al. (1989). Only  $M_2$  was observed in samples from the Malrok zone, probably because its high metamorphic grade obliterated the first event ( $M_1$ ). Metamorphic grade increases to the west from lower and upper amphibolite facies (Ridge Lake) marked by the assemblages stilpnomelane-garnet-amphibole, biotite-garnet-amphibole, or amphibole-clinopyroxene. The highest metamorphic grade corresponds to granulite facies (Malrok), evidenced by the assemblage fayalite-orthopyroxene-clinopyroxene, although fayalite was identified in only one sample. The most common assemblage of orthopyroxene-clinopyroxene-grunerite, corresponds to the transition from amphibolite to granulite facies. Partial melting or migmatization, a common process present

in high-grade metamorphism, was not observed in thin section, but its absence can be explained in terms of the relative abundance of  $H_2O$  and  $CO_2+N_2$  (Butcher and Frey, 2002, Fig. 9.8). Schists and gneisses commonly exhibit planar fabrics parallel to bedding ( $S_0$ ), defined by the orientation of amphiboles, biotite, or by bands with different mineral assemblages or differences in the proportion of minerals. Original structures from the sedimentary protolith are usually well preserved in spite of the metamorphic grade, suggesting that metamorphism was not accompanied by significant shear deformation. However, slightly rotated inclusion trails in garnets porphyroblasts imply that garnet growth during prograde metamorphism ( $M_2$ ) is contemporaneous with either  $D_2$  or  $D_3$  deformational events. Significant overprint of preexisting structures during the widespread  $M_2$  metamorphic event makes the relation between  $M_1$  and  $D_1$  unclear and hard to define in this study.

Talc, chlorite, serpentine (or anhedral stilpnomelane), calcite, epidote, and probably green biotite represent common retrograde minerals in almost all samples, although they appear only in very small modal abundances. They were probably formed during the third ( $D_3$ ) deformational event (Henderson et al., 1989; Corrigan et al., 2001).

*Banded Iron Formations:* Metamorphism produced the current mineralogy in the project area, and it has affected silicate-rich and sulfide-rich BIFs differently. Silicate-rich BIF is characterized by assemblages of orthopyroxene-clinopyroxene at Malrok and amphibole-garnet-biotite at Ridge Lake. These assemblages reflect the difference in metamorphic grade between the two areas, which is higher at Malrok. Silicate-rich BIF is the most common type and sulfides, where locally abundant, are always interbedded with silicate facies. Probably the most widespread and evident effect of metamorphism in sulfides is recrystallization, though refractive arsenopyrite does not show such changes.

It is evident that at least some, if not all mineralization occurred post peak-metamorphism because pyrrhotite, chalcopyrite, and minor sphalerite are locally crosscutting metamorphic fabric and fractures in silicates, especially garnet. On the other hand, the possibility that mineralization has occurred before the last metamorphic event cannot be precluded, and that some remobilization of sulfides took place later. Noteworthy, however, is the absence of evidence that refractive sulfides (i.e., arsenopyrite) crosscut silicates or foliation. Sulfidation, or more exactly pyrrhotitization, occurred at the expense of pyrite, magnetite, and probably ilmenite, since

replacement textures have been identified in some samples. Conclusive mineralogical confirmation for the origin as either epigenetic or syngenetic is still incomplete, but replacement evidence and crosscutting features support an epigenetic source for gold mineralization; moreover, no deformation of pyrrhotite and arsenopyrite has been identified after sulfide deposition.

### *Retrograde Metamorphism*

Retrograde metamorphism is incipient in most samples and is characterized by: garnet replaced by chlorite-calcite-epidote; amphiboles replaced by calcite-chlorite; amphiboles and pyroxenes replaced by serpentine; fractures in silicates and metamorphic fabric filled with serpentine; inter-grain spaces filled with calcite; and probably brown biotite locally converted to green biotite.

Retrograde metamorphism can be confused with hydrothermal alteration because assemblages such as calcite-chlorite-epidote are similar to those present in some alteration types, and a small amount of gold is associated with retrograde minerals (Table 4). However, spatial relations such as vein selvages or lateral transitions to these assemblages were not identified in studied samples, instead, these minerals are randomly alter prograde silicate minerals.

### **Mineralization**

The bulk of mineralization occurs in sulfide-rich bands (at least at meso- and micro-scale) and is more common in silicate-rich BIFs, and frequently associated with garnet-rich bands. The later can be interpreted as unique remnants of the original mineralogy prior mineralization, if sulfidation occurred post peak-metamorphism. Disseminated sulfides are also abundant and likewise are more abundant in silicate-rich BIFs. By far the most abundant sulfide is pyrrhotite, which appears in massive mosaic-like textures, typically in millimetric bands. Minor amounts of chalcopyrite are present as inclusions in pyrrhotite, and single grains of sphalerite are also associated with it. Pyrrhotite seems to have replaced magnetite, ilmenite, and pyrite. Bigger euhedral arsenopyrite grains are present locally associated with specific bands, and frequently are cored by irregular relicts of gold-bearing loellingite. Most gold is present as inclusions accompanied by minor amounts of native bismuth and maldonite inclusions within loellingite. No galena was found. In general, the base-metal content in these samples is low, which is typical of BIFs (Klein, 2005).

### *Preminalization*

Magnetite and ilmenite have been identified as mineral phases present before sulfidation. It is very likely that pyrite had been present during diagenesis and that pyrite was the source of sulfur for pyrrhotite during metamorphism; however, there are very few examples of what could be relicts of pyrite. In only one sample was a pyrrhotite grain observed that is cored by relicts of magnetite and pyrite.

### *Mineralization Sequence*

Two main mineralization events have been identified in BIFs in the Malrok and Ridge Lake zones. Each event has specific characteristics and occurred at different times, but they could have happened as a single and continuous process, though not simultaneously. Gold deposition is more associated with the first event, where it is more abundant; however, it may be occurred just in the transition from the first to the second event because it is always found in the limit of the two characteristic minerals of each event (see very low and low sulfidation events).

*Very low sulfidation:* The first event has a very low sulfidation state, characterized by the presence of loellingite that always occurs as relictic cores in euhedral arsenopyrite from the second event. Loellingite is an arsenide of iron ( $\text{FeAs}_2$ ) and has minor amounts of nickel and cobalt (Figs. 15 and 16) within its mineral structure (up to 5.5 weight percent of nickel and 2.1 weight percent of cobalt). Gold is closely associated with loellingite, where it appears as inclusions near the border of single grains. Inclusions of native bismuth and maldonite (bismuthide of gold,  $\text{Au}_2\text{Bi}$ ) go together with gold in minor amounts. This mineral association allows constrain of sulfidation state and temperature as observed in Figure 23. It has been impossible, however, to establish the temporal relationship between this first event and any specific metamorphic event, because all minerals from this event are surrounded by euhedral arsenopyrite from the second event.

*Low sulfidation:* The later mineralization event was more abundant in sulfur, in a low sulfidation state (Fig. 23), characterized by replacement of magnetite, ilmenite, and probably pyrite, by pyrrhotite (Fig. 13). Related with this event are frequent inclusions of chalcopyrite in pyrrhotite and trace amounts of sphalerite (Fig. 14). Euhedral arsenopyrite is associated with this event, but it is commonly surrounded by massive mosaics of pyrrhotite, what could be evidence that

arsenopyrite was deposited early in this event. This sulfide is cored by irregular relicts of loellingite that sometimes has inclusions of gold near its borders, as mentioned before.

#### *Remobilization or post peak-metamorphic mineralization?*

Non-refractory sulfides such as pyrrhotite commonly occur in fractures of garnet (Fig. 12) and surrounding it, or crosscutting the metamorphic fabric; this implies at least local remobilization of sulfides or that either part or all of the gold mineralization occurred post peak-metamorphism. Minor gold was also locally remobilized in this event, but it is likely that refractory arsenopyrite endured through this process, protecting cores that largely consist of loellingite and most gold inclusions in it. Local remobilization of gold may cause it also to be associated with other sulfides, such as pyrrhotite or as free gold associated with metamorphic silicates (Fig. 14). Petrographic study of these rocks is not sufficient to establish conclusively the relative timing of gold mineralization and metamorphism.

#### *Incipient pyritization*

Very uncommon pyrite is found in pyrrhotite fractures replacing it. This is the very last, though incipient evidence for precipitation of sulfides in the studied samples, but has been found very locally and incipiently to assure that this is a regional process.

### **Comparison with Other Gold-Bearing BIF Deposits Worldwide**

Among the most important gold-bearing BIFs worldwide are Homestake, South Dakota, U.S.A.; Agnico-Eagle, Quebec, Canada; Lupin, Northwestern Territories, Canada; Mt. Morgans, Yilgarn Block, Australia; Vubachikwe and other minor mines, Gwanda greenstone belt, Zimbabwe; and Sao Bento, Cuiaba, and Morro Velho mines in Minas Gerais, Brazil (Table 5). These are geographically widespread deposits, though they are restricted to greenstones belts and other supracrustal sequences. This section compares several geologic characteristics of these deposits with observations made in the Malrok and Ridge Lake samples.

Most gold-bearing BIFs are Archean in age but Homestake Formation in the Homestake mine is Early Proterozoic, as the Bravo Lake Formation in central Baffin Island, and both correspond with the Trans-Hudson Orogeny in northeastern U.S.A. and Canada. The mineralogy depends on the BIF facies, but common iron-rich minerals are silicates such as grunerite, minnesotaite, and

almandine; carbonates like ankerite and siderite; oxides such as magnetite and hematite; and sulfides such as pyrite and pyrrhotite. Frequently, more than one facies are present and mostly depend on depositional environment and/or epigenetic replacement. Volcanic and volcanoclastic strata are interstratified with pelites and chemical sedimentary rocks, in some cases intruded by mafic and ultramafic dikes and sills, as is the case in the Bravo Lake Formation.

Although gold is related with sulfides in all deposits, gold-bearing BIF facies are quite variable from carbonate-rich BIFs in the Homestake, Agnico-Eagle, and Cuiaba mines and in the Gwanda greenstone belt; oxide facies in the Mt. Morgans mine; and silicate facies in the Lupin mine and in the Malrok and Ridge Lake prospects. All deposits have variable proportions of sulfide facies; however, in some places such as Mt. Morgans and in this work, those sulfides are interpreted to be the replacement products of other BIF facies, for example iron oxides.

Deformational and metamorphic events are highly variable as well. The Agnico-Eagle mine, only one deformational event is reported whereas deposits such as Mt. Morgans and Morro Velho have undergone four deformational events. Other deposits report two or three and in Baffin Island at least three have been recognized (Henderson et al., 1989). Medium to high metamorphic grade is present in the Lupin mine and was identified in this work, but most deposits of this type are hosted in lower grade rocks of greenschist and lower amphibolite facies. This complexity in deformational and metamorphic history in these deposits makes the assessment of the genesis of BIF ores very difficult. It is noteworthy to point out again that the only two Early Proterozoic deposits, Homestake and Baffin Island (this work), are both associated with the Trans-Hudson Orogeny, in the north eastern part of North America.

Some characteristics that argue in favor of an epigenetic origin for these deposits are the structural control on mineralization, alteration that may be hydrothermal, and replacement textures. All deposits show at least some ore control among hinges of folds, fault and shear zones, and, in some cases, gold is restricted to quartz and/or carbonate veins. Chlorite, sericite, and carbonates are alteration minerals or vein halos in some deposits (Homestake, Sao Bento, Mt. Morgans, and Cuiaba), whereas in others, alteration evidence has not been identified (Morro Velho and this work). On the other hand, sulfidation is common in most gold-bearing BIFs (including Malrok and Ridge Lake) and is interpreted as a replacement process mostly of oxide facies.

Without exception, most gold mineralization in these deposits is strongly related with sulfides such as pyrite, pyrrhotite, and/or arsenopyrite; however, only at Lupin and in this work has it been reported that an important place for gold deposition is at the boundary between cores of loellingite and surrounding euhedral arsenopyrite.

Gold to silver ratios has been suggested as a distinctive parameter for differentiating between stratiform and non-stratiform (i.e., vein-type) BIFs (Kerswill, 1995). Typically, Au:Ag ratio in stratiform-type deposits is around 5.0, whereas vein-type deposits have a ratio of more than 8.0. Only a few grains were analyzed in samples from the Malrok and Ridge Lake prospects, but it seems that gold in sulfides varies between ca. 3.0 and 6.0, whereas free gold in silicates has a higher ratio, ca. 40.0. As data are very few is impossible to make conclusive observations, but these differences could indicate multiple sources for gold at Baffin Island.

Finally, gold content is highly variable, from hundreds of thousands of ounces to several millions of ounces, though exceptional deposits such as Homestake and Morro Velho have 40 and 16 million ounces, respectively.

### **Exploration Implications**

Regardless of the controversies between syngenetic and epigenetic origin of sulfides and gold mineralization, the occurrences appear to have lateral continuity, at least at meso-scale (hand sample and thin section), and this implies that stratigraphic controls on mineralization are at least locally important and cannot be underestimated, even in the epigenetic scenario. However, evidence of at least some remobilization of sulfides, if not the bulk of mineralization, after the last metamorphic event implies that large structures such as faults, discontinuities, or shear zones are likely sites for gold transport and deposition. In other words, both stratigraphic and structural traps have to be assessed simultaneously.

As gold appears mostly as inclusions in loellingite, arsenic is expected to be the best pathfinder element for regional exploration. As bismuth, nickel, and cobalt are also associated with loellingite, they can be good pathfinders, but in a secondary role.

Minor amounts of gold were found as inclusions in arsenopyrite or pyrrhotite, and as free gold with silicates, so arsenic should not be the only geochemical criterion for regional gold exploration.

### **Possibilities for Future Works**

The most important future work that can be made is a comparison between observations and results of this petrographic work and field work and logging on Baffin Island. In this way, the continuity of sulfide BIF on Baffin Island can be studied to find indications of the nature of mineralization at a regional scale.

More detailed microprobe analyses can provide the basis for calculating the temperature and pressure conditions of peak-metamorphism, as Gole and Klein (1981) discussed for high metamorphic grade BIFs in Western Australia.

REE studies can provide evidence regarding the origin of hydrothermal sources of iron in BIF (e.g., deep-ocean hydrothermal input; Klein and Ladeira, 2000).

Comparisons of REE contents between mineralized and barren BIF with similar mineralogy can indicate a probable source for gold. For instance, Saager et al. (1987) show a decreasing trend in REE in a gold-bearing BIF, whereas Klein (2005) indicates an increasing trend for gold-barren BIFs. These observations can be arguments for a different source of each type of BIF, one epigenetic and other syngenetic.

Other comparisons that may be done are with whole-rock geochemical analyses of BIFs to contrast them with the composition of rocks presently venting on the sea floor, such as black smokers.

Fluid inclusions might be important to analyze the volatile content, salinity, and origin of fluids and the T and P of trapping, although metamorphism and deformation provide challenges for interpretation.

The age of mineralization can be obtained with Re-Os techniques in arsenopyrite, other sulfides, and gold, because this system has a high closure temperature, is expected not to be affected by metamorphic processes. Example of this analysis was made by Morelli et al. (2005) at Homestake mine, in South Dakota.

Re-Os analyses allow also an assessment of the sources of iron, sulfur, and gold. Common or different sources can be identified with these types of studies, although the presence of multiple geologic events provides challenges for interpretation.

### **Summary and Conclusions**

In central Baffin Island several Banded Iron Formations (BIFs) have been identified within the Early Proterozoic Bravo Lake Formation. In this paper, two of them are described: Malrok and Ridge Lake. BIFs are characterized by assemblages of orthopyroxene + clinopyroxene + grunerite ± almandine ± fayalite in the case of Malrok, and grunerite + clinopyroxene + ferro-actinolite + garnet or biotite + garnet ± amphibole at Ridge Lake. These assemblages represent the metamorphic grade of each prospect, high grade in granulite facies in Malrok and medium grade in amphibolite facies at Ridge Lake. Two metamorphic events were identified petrographically, in agreement with observations made by other authors; retrograde metamorphism postdates these two prograde events.

In the present study, alteration that may indicate the presence of a hydrothermal fluid has not been identified in the studied samples; moreover, alteration and metamorphic products of retrograde metamorphism are sometimes similar, i.e., chlorite or epidote. As the occurrence of these minerals is not associated with any structure or veins selvage, they are interpreted to be retrograde nature, though minor gold associated with these retrograde minerals may imply that they have relevance for gold deposition.

Two mineralization events were identified, but gold is most related with the first one, or as a transition between them, occurring mostly as inclusions in loellingite from the first event. This mineral association allows some constraints on the temperature range and sulfidation state of gold deposition, given by the stability of loellingite. The second event could have remobilized some minor amounts of gold or could have brought in gold independently. This second event may have been produced by pyrrhotitization of pyrite, magnetite, and ilmenite, probably during peak-metamorphism. Arsenopyrite replacing and/or surrounding loellingite accompanied this event, and arsenopyrite is almost always surrounded or accompanied by mosaics of pyrrhotite. Chalcopyrite mostly occurs as inclusions in pyrrhotite, which indicates that both are related to the

same mineralization event. Ilmenite is more common in sulfide-depleted wall-rocks, which could imply that pyrrhotite is replacing it where sulfides are abundant.

The timing of both mineralization events with respect to different metamorphic events remains elusive because it seems that at least some remobilization of sulfides, if not the entire mineralization event, occurred after the last episode of metamorphism, making it impossible to recognize conclusive temporal relationships between metamorphic silicates and sulfides before this episode. Moreover, medium- to high-grade metamorphism may have completely obliterated prior relationships or evidence of syngenetic mineralization.

As evidence for epigenesis or syngeneses is still inconclusive, exploration has to be focused on both possibilities, in other words, stratigraphy (sulfide-rich BIFs) and structures (faults, discontinuities, or shear zones) have to be evaluated together in order to make a good assessment for the presence or absence of gold mineralization.

Arsenic continues to be the most important pathfinder mineral, but bismuth, nickel, and cobalt have to be considered also, as they are highly associated with gold-bearing loellingite. Sulfur and copper can also be good indicators, but on a more regional scale, because they are not directly associated with gold.

Complementary field work and core logging have to be done to compare results of this study with field-scale characteristics of mineralization.

### **Acknowledgments**

I want to thank AngloGold Ashanti and Commander Resources for their data and financial support for this work. I want to also thank my committee members, Eric Seedorff, Mark Barton, and Spencer Titley, and also to Frank Mazdab, Lukas Zurcher, and the Economic Geology group of the University of Arizona for their assistance and comments.

### **References**

Barton, P., and Skinner, B., 1979, Sulfide mineral stabilities, *in* Barnes, H., ed., *Geochemistry of Hydrothermal Ore Deposits*: New York, John Wiley and Sons, p. 278-403.

Bethune, K., and Scammell, R., 2003, Geology, geochronology, and geochemistry of Archean rocks in the Ege Bay area, north-central Baffin Island, Canada: Constraints on the depositional and tectonic history of the Mary River Group of northeastern Rae Province: Canadian Journal of Earth Sciences, v. 40, p. 1137-1167.

Bullis, H., Hureau, R., and Penner, B., 1993, Distribution of gold and sulfides at Lupin, Northwest Territories: Economic Geology, v. 89, p. 1217-1227.

Butcher, K., and Frey, M., 2002, Petrogenesis of Metamorphic Rocks, 7th ed.: Berlin, Springer, 341 p.

Caddey, S., Bachman, R., Campbell, T., Reid, R., and Otto, R., 1991, The Homestake gold mine, an Early Proterozoic iron-formation-hosted gold deposit, Lawrence County, South Dakota: U. S. Geological Survey Bulletin 1857-J, p. 1-67.

Castro, L., 1994, Genesis of banded iron-formations: Economic Geology: v. 89, p. 1384-1397.

Colvine, A., 1988, Gold mineralization in the Superior Province, Canada, a product of terminal Archean cratonization, *in* Goode, A., and Bosma, L., eds., Bicentennial Gold '88, Extended Abstracts, Oral Programme: Geological Society of Australia, Abstracts Series no. 22, p. 36-44.

Corrigan, D., Scott, D., and St-Onge, M., 2001, Geology of the northern margin of the Trans-Hudson Orogeny (Foxe Fold Belt), central Baffin Island, Nunavut: Current Research Geological Survey of Canada, Report No. 2001-C23, 27 p.

Einaudi, M., Hedenquist, J., and Inan, E., 2003, Sulfidation state of fluids in active and extinct hydrothermal systems: Transitions from porphyry to epithermal environments: Economic Geology Special Publication No. 10, p. 285-313.

Fripp, R., 1976, Stratabound gold deposits in Archean banded iron-formation, Rhodesia: Economic Geology, v. 71, p. 58-75.

Fyon, J., Crocket, J., and Schwarcz, H., 1983, The Carshaw and Malga iron-formation-hosted deposits of the Timmins area: Ontario Geological Survey, Miscellaneous Paper 110, p. 98-110.

Gole, M., and Klein, C., 1981, High-grade metamorphic Archean banded iron-formations, Western Australia: Assemblages with coexisting pyroxenes-fayalite: *American Mineralogist*, v. 66, p. 87-99.

Goldfarb, R., Baker, T., Dube, B., Groves, D., Hart, C., and Gosselin, P., 2005, Distribution, character, and genesis of gold deposits in metamorphic terranes: *Economic Geology 100th Anniversary Volume*, p. 407-450.

Groves, D., Phillips, S., Ho, S., Henderson, M., Clark, M., and Woad, G., 1982, Controls on distribution of Archean hydrothermal gold deposits in Western Australia, *in Foster, R. P., ed., Gold '82; The Geology, Geochemistry and Genesis of Gold Deposits: Rotterdam, Balkema*, p. 689-712.

Groves, D., Phillips, G., Falconer, L., Houston, S., Browning, P., and Dahl, N., 1988, BIF-hosted gold deposits in Archean greenstone belts of Western Australia; Evidence for an epigenetic origin: *Krystalinikum*, v. 19, p. 91-109.

Henderson, J., Grocott, J., Henderson, S., and Perreault, S., 1989, Tectonic history of the Lower Proterozoic Foxe-Rinkian Belt in central Baffin Island, N.W.T.: *Geological Survey of Canada, Paper v. 89-1C*, p. 185-197.

Hodgson, C., and MacGeehan, P., 1982, Geological characteristics of gold deposits in the Superior Province of the Canadian Shield, *in Hodder, R. W., and Petruk, W., eds., Geology of Canadian Gold Deposits: Canadian Institute of Mining and Metallurgy Special Volume 24*, p. 211-229.

Hoffman, P., 1988, United Plates of America, the birth of a craton; Early Proterozoic assembly and growth of Laurentia: *Annual Reviews of Earth and Planetary Sciences*, v. 16, p. 543-603.

Hutchinson, R., 1976, Lode gold deposits: The case for volcanogenic distribution, *in Pacific Northwest Mining and Metals Conference., Portland, Oregon, 1975, Proceedings: Salem, Oregon Department of Geology and Mineral Industries*, p. 64-105.

Hutchinson, R., Ridler, R., and Suffel, G., 1971, Metallogenic relationships in the Abitibi belt, Canada: A model for Archean metallogeny: *Canadian Institute of Mining and Metallurgy, Trans.*, v. 74, p. 106-115.

James, H., 1954, Sedimentary facies of iron-formation: *Economic Geology*, v. 49, p. 235-293.

Kerswill, J., 1995, Iron-formation-hosted stratabound gold, *in* Eckstrand, O., Sinclair, W., and Thorpe, R., eds., *Geology of Canadian Mineral Deposits Types: Geological Survey of Canada, Geology of Canada, No. 8*, p. 367-382.

Klein, C., 2005, Some Precambrian banded iron-formations (BIFs) from around the world: Their age, geologic setting, mineralogy, metamorphism, geochemistry, and origin: *American Mineralogist*, v.90, p. 1473-1499.

Klein, C., and Ladeira, E., 2000, Geochemistry and petrology of some Proterozoic banded iron-formations of the Quadrilatero Ferrifero, Minas Gerais, Brazil: *Economic Geology*, v. 95, p 405-427.

Leake, E., Woolley, A., Arps, C., Birch, W., Gilbert, C., Grice, J., Hawthorne, F., Kato, A., Kisch, H., Krivovichev, V., Linthout, K., Laird, J., Mandarino, J., Maresch, W., Nickel, E., Rock, N., Schumacher, J., Smith, D., Stephenson, N., Ungaretti, L., Whittaker, E., and Guo, Y., 1997, Nomenclature of amphiboles; Report of the Subcommittee on Amphiboles of the International Mineralogical Association, Commission on New Minerals and Mineral Names: *Canadian Mineralogist*, v. 35, p. 219-246.

Martins, S., Lobato, L., Ferreira, J., and Jardim, E., 2007, Nature and Origin of the BIF-hosted Sao Bento gold deposit, Quadrilatero Ferrifero, Brazil, with special emphasis on structural controls: *Ore Geology Reviews*, v. 32, p. 571-595.

Morelli, R., Creaser, R., and Bell, C., 2005, Re-Os arsenopyrite geochronology of the Homestake gold deposit, Black Hills, South Dakota, and implications for chronometer closure temperature [abs.]: *Geological Society of America Abstracts with Programs*, v. 37, p. 452.

Nelson, G., 1985, Gold mineralization at the Homestake gold mine, Lead, South Dakota: *Canadian Institute of Mining and Metallurgy Bulletin*, v. 1974-78, 879, p. 38.

Phillips, G., Groves, D., and Martyn, J., 1984, An epigenetic origin for Archean banded iron-formation-hosted gold deposits: *Economic Geology*, v. 79, p. 162-171.

Phillips, G., Groves, D., and Martyn, J., 1984, An Epigenetic Origin for Archean Banded Iron-Formation-Hosted Gold Deposits: *Economic Geology*, v. 79, p. 162-171.

Ribeiro, L., Friedrich, G., Chemale, F., Oliveira, C., Carmo, V., and Vieira, F., 1998, Structural evolution and genesis of the Archean BIF-hosted Cuiaba old mine, Minas Gerais, Brazil: Symposium on Latin-American Geosciences, 15th, Brazil, 16 October, Proceedings, p. 751-765.

Ribeiro, L., Oliveira, G., and Friedrich, G., 2007, The Archean BIF-Hosted Cuiaba gold deposit, Quadrilatero Ferrifero, Minas Gerais, Brazil: *Ore Geology Reviews*, v. 32-3-4, p. 543-570.

Ridler, R., 1970, Relationship of mineralization to volcanic stratigraphy in the Kirkland-Larder Lakes area, Ontario: Geological Association of Canada Annual Meeting, Proceedings, v. 21, p. 33-42.

Saager, R., Oberthuer, T., and Tomschi, H., 1987, Geochemistry and mineralogy of banded iron-formation-hosted gold mineralization in the Gwanda greenstone belt, Zimbabwe: *Economic Geology*, v. 82, p. 2017-2032.

Salier, B., Groves, D., McNaughton, N., and Fletcher, I., 2005, Geochronological and stable isotope evidence for widespread orogenic gold mineralization from a deep-seated fluid source at ca 2.65 Ga in the Laverton gold province, Western Australia: *Economic Geology*, v. 100, p. 1363-1388.

Schumacher, J. C., 1997, Appendix 2. The estimation of the proportion of ferric iron in the electron-microprobe analysis of amphiboles, *in* Leake, B. E., et al., 1997, Nomenclature of Amphiboles: Report of the Subcommittee on Amphiboles of the International Mineralogical Association, Commission on New Minerals and Mineral Names: *Canadian Mineralogist*, v. 35, p. 238-246.

Scott, D., St-Onge, M., and Corrigan, D., 2003, Geology of the Archean Rae Craton and Mary River Group and the Paleoproterozoic Piling Group, central Baffin Island, Nunavut: Current Research Geological Survey of Canada, Report No. 2003-C26, p.12.

Slack, J., and Cannon, W., 2009, Extraterrestrial demise of banded iron formations 1.85 billion years ago: *Geology*, v. 37; no. 11, p. 1011-1014.

Slack, J., Grenne, T., Bekker, A., Rouxel, O., and Lindberg, P., 2007, Suboxic deep seawater in the Late Paleoproterozoic: Evidence from hematitic chert and iron formation related to seafloor-hydrothermal sulfide deposits, central Arizona, USA: *Earth and Planetary Science Letters*, v. 255, p. 243-256.

S Spear, F., 1995, Metamorphic phase equilibria and pressure-temperature-time paths, 2<sup>nd</sup> (Corrected) Printing: Washington, D. C., Mineralogical Society of America, 799 p.

Stacey, J., 2005, Geology and metallic mineralization of a representative klippe of the Bravo Lake Formation, Baffin Island, Nunavut: Unpublished M. Sc. thesis, Alberta, Canada, The University of Calgary, 318 p.

Stacey, J., and Pattison, D., 2003, Stratigraphy, structure, and petrology of a representative klippe of the Bravo Lake Formation, Piling Group, central Baffin Island, Nunavut: Current Research Geological Survey of Canada, Report No. 2003-C13, p. 11.

Taylor, F., 1982, Precambrian geology of the Canadian North Borderlands, *in* Kerr, J., Ferguson, A., and Machan, L., eds., *Geology of the North Atlantic Borderlands: Canadian Society of Petroleum Geologists, Memoir 7*, p. 11-30.

Valliant, R., and Hutchinson, R., 1982, Stratigraphic distribution and genesis of gold deposits, Bousquet Region, northwestern Quebec, *in* Hodder, R. W., and Petruk, W., eds., *Geology of Canadian Gold Deposits: Canadian Institute of Mining and Metallurgy Special Volume 24*, p. 27-40.

Vieira, F., Lisboa, L., Chaves, J., de Oliveira, G., Clemente, L., and de Oliveira, R., 1991, Excursion to the Morro Velho gold mine, Minas Gerais, Brazil, *in* Thorman, C., Ladeira, E., and Schnabel, D., eds., *Gold Deposits Related to Greenstone Belts in Brazil: U. S. Geological Survey Bulletin 1980-A*, p. A67-A73.

Vielreicher, R., Groves, D., Ridley, J., and McNaughton N., 1994, A replacement origin for the BIF-hosted gold deposit at Mt. Morgans, Yilgarn Block, W.A.: *Ore Geology Reviews*, v. 9, p. 325-347.

Wyman, D., Kerrich, R., and Fryer, B., 1986, Gold mineralization overprinting iron formation at the Agnico-Eagle deposit, Quebec, Canada: Mineralogical, microstructural and geochemical evidence, *in* Macdonald, A. J., ed., *Proceedings of Gold '86 , an International Symposium on the Geology of Gold*, , Toronto, p. 108-123.

Wodicka, N., St-Onge, M., Scott, D., and Corrigan, D., 2002, Preliminary report on the U-Pb geochronology of the northern margin of the Trans-Hudson orogen, central Baffin Island: Current Research Geological Survey of Canada, Report No. 2002-F7, p. 12.

Figures

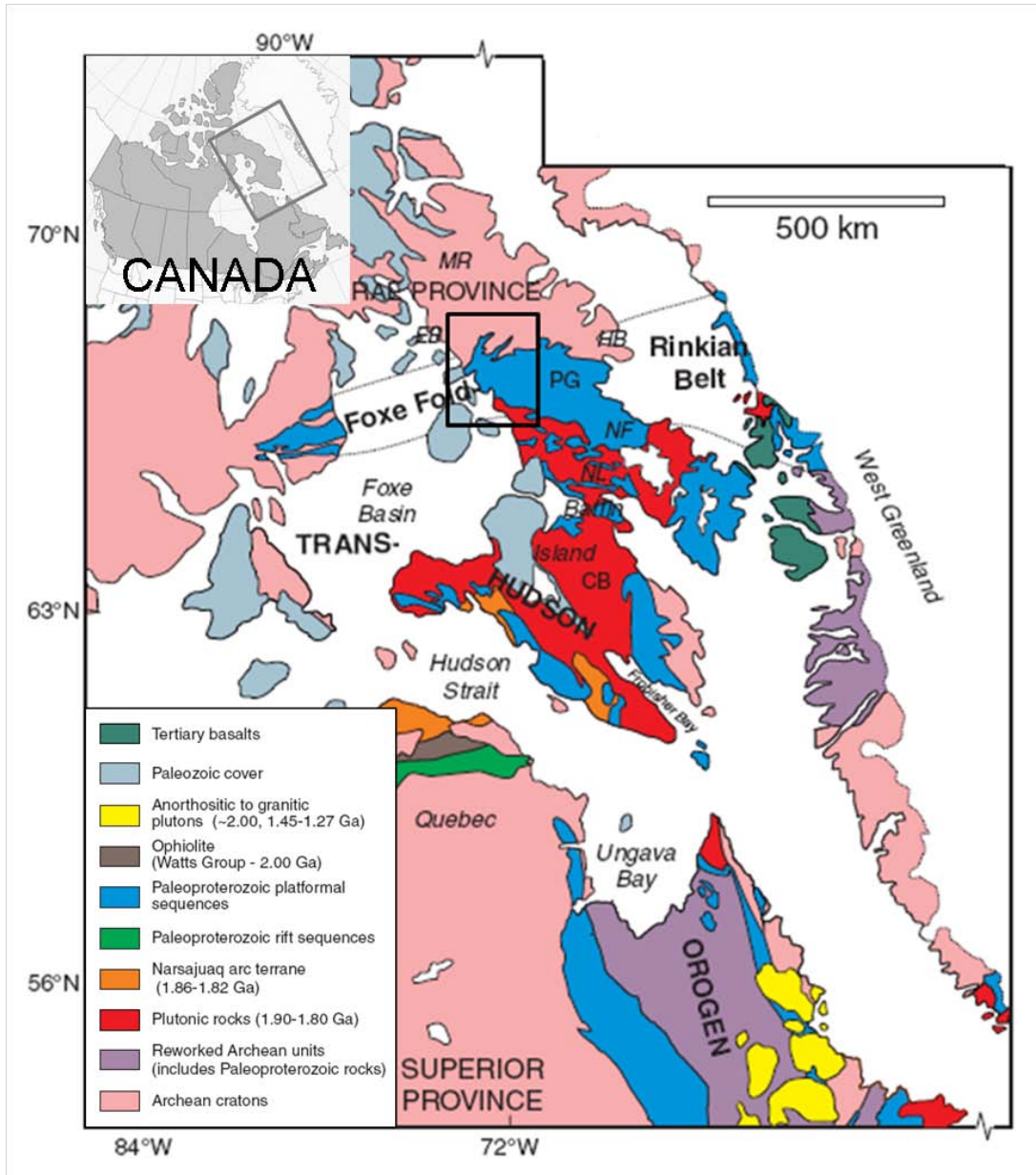


Figure 1: Location and generalized geology of part of northeastern Canada, Baffin Island, and western Greenland. Note the position of the Foxe Fold Belt and its correlation with the Rinkian Belt in Greenland. Plutonic rocks intrude the Pilling Group and can constrain its age. Black box outlines Figure 2. After Wodicka et al. (2002).

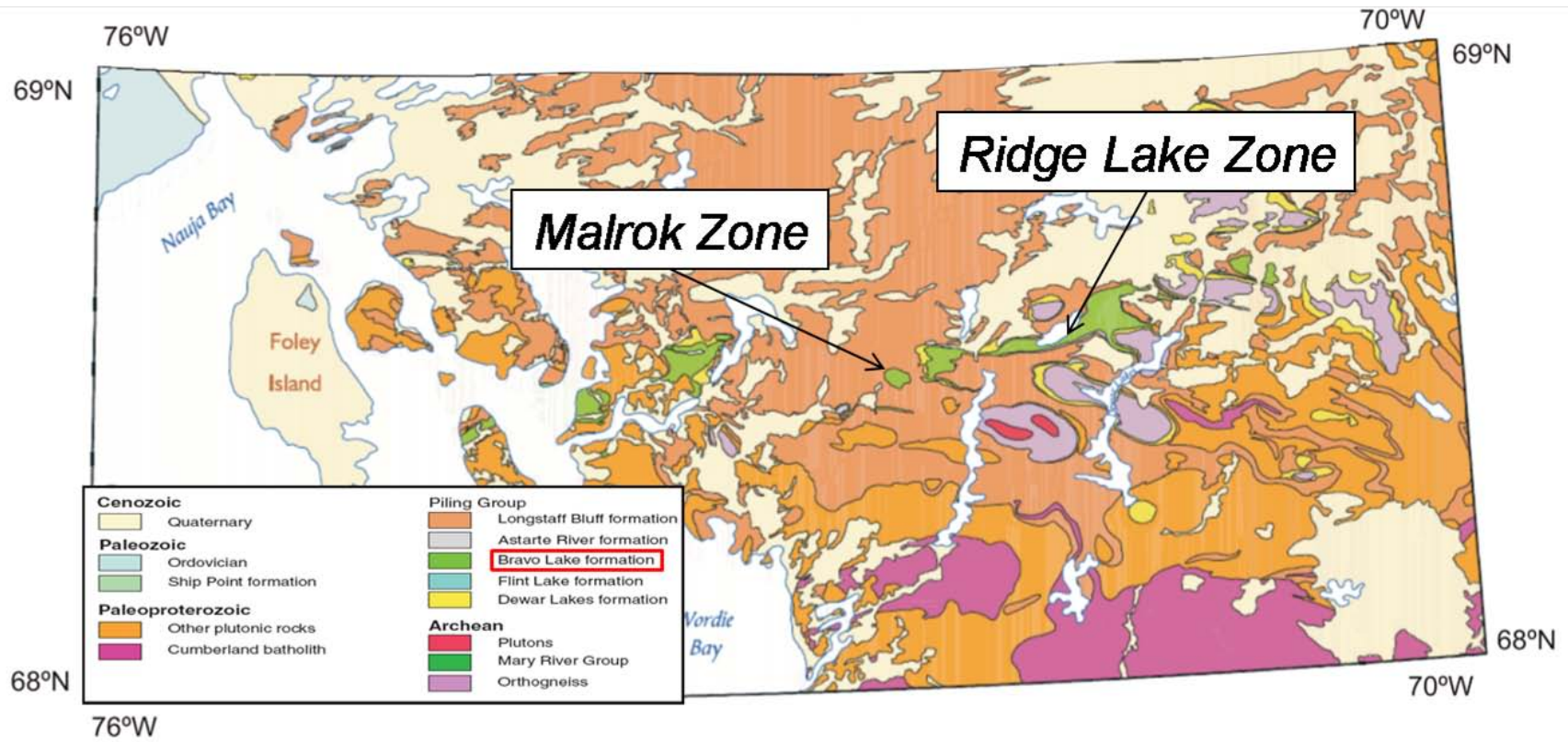


Figure 2: Generalized geology of central Baffin Island and location of the two exploration prospects. After Scott et al. (2002).

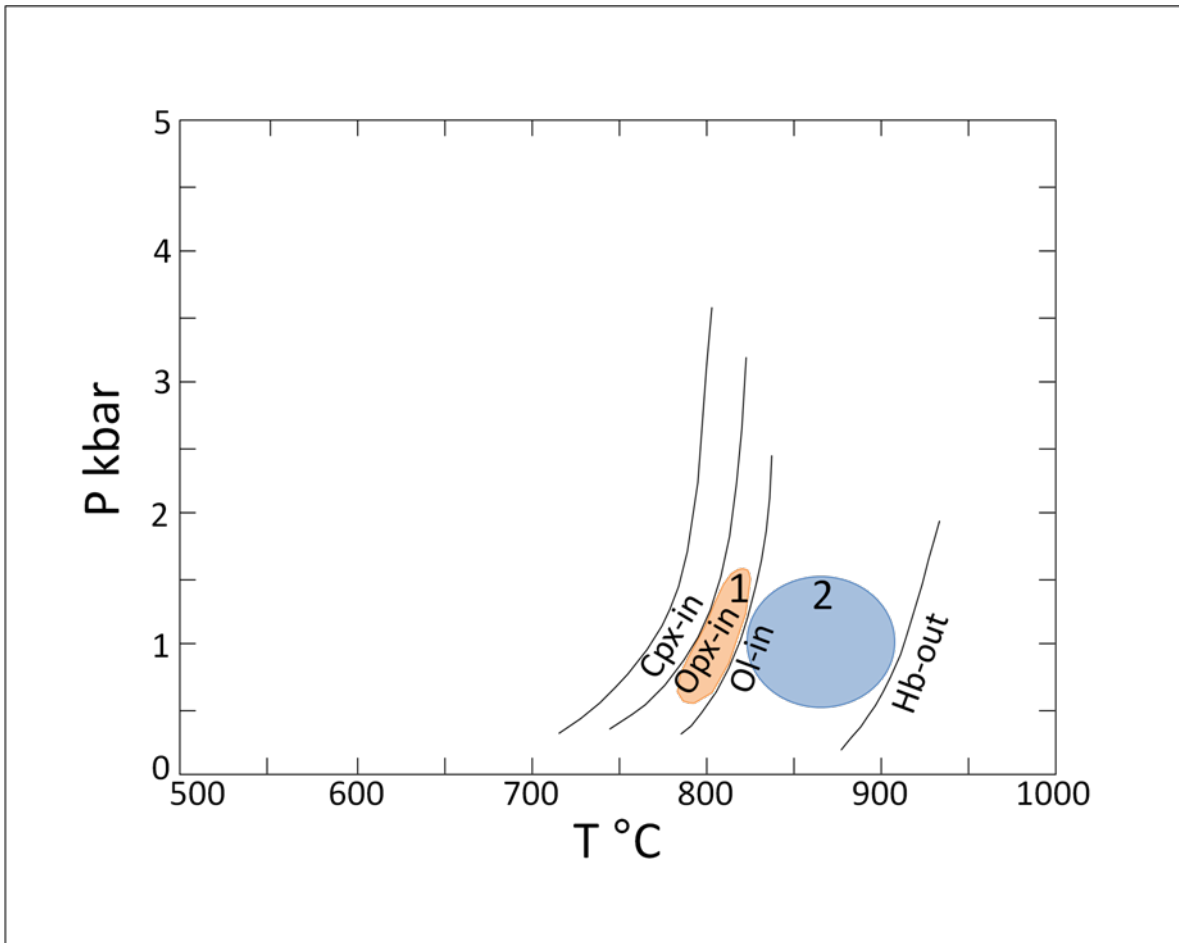


Figure 3: P-T diagram showing the P-T conditions of reaction boundaries pertinent to the amphibolite to granulite facies transition. Curves are for  $fO_2$  conditions defined by the quartz – fayalite – magnetite (QFM) buffer. Number 1 represent most samples from the Malrok zone, where the typical assemblage is clinopyroxene + orthopyroxene + amphibole; number 2 represent a higher metamorphic grade sample where fayalite was identified. After Spear (1995).

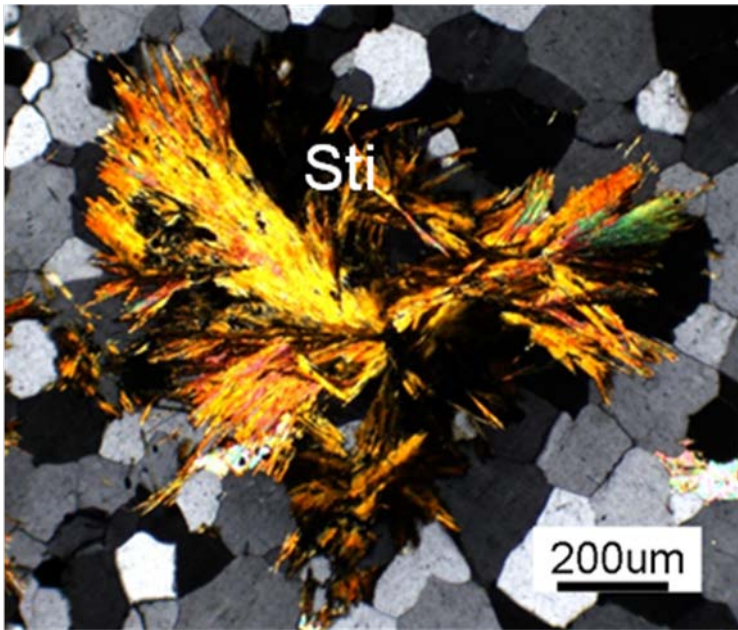


Figure 4: An aggregate of prograde stilpnomelane (Sti) needles surrounded by recrystallized quartz. Ridge Lake. Photomicrograph, transmitted cross polarized light.

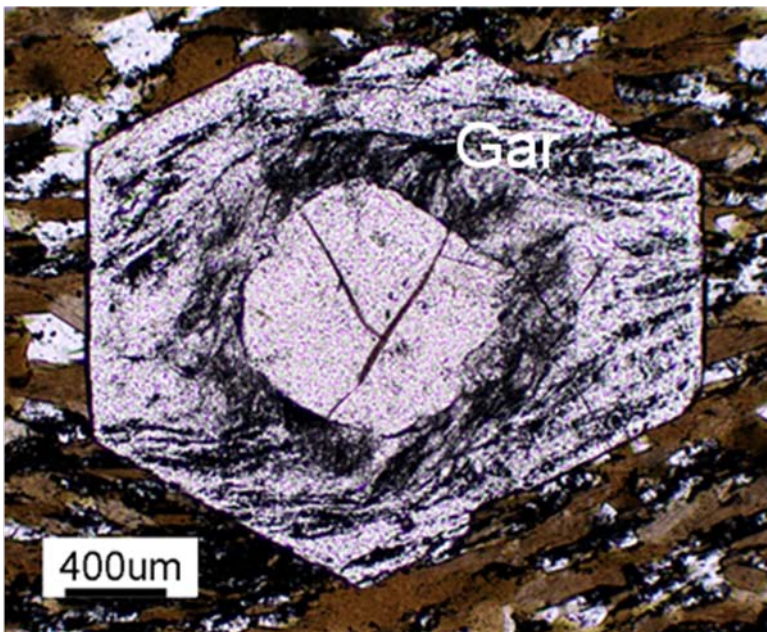


Figure 5: Post-metamorphic garnet (Gar) with a pre-metamorphic core. Ridge Lake. Photomicrograph, transmitted plane polarized light.

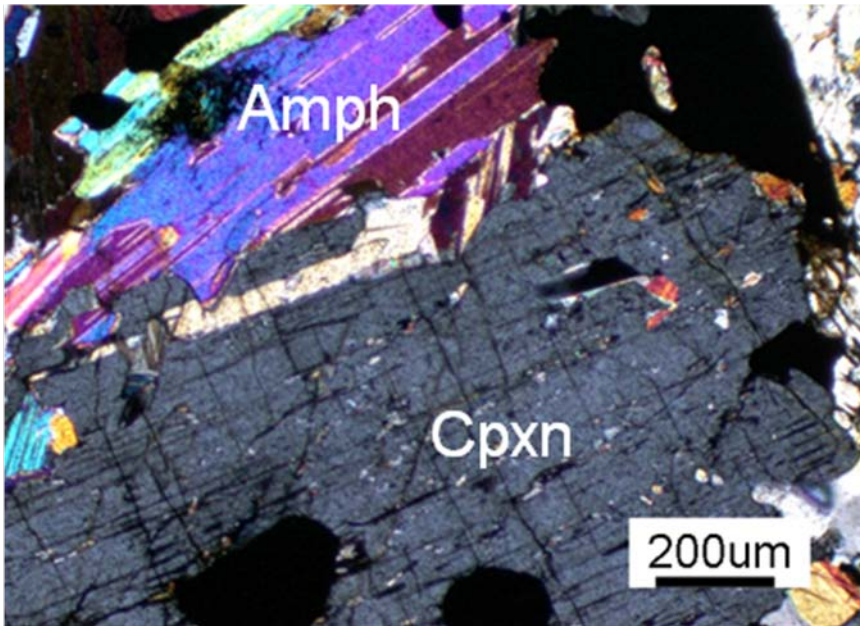


Figure 6: Orthopyroxene (Opxn) in equilibrium with amphibole (Amph). Malrok. Photomicrograph, transmitted cross polarized light.

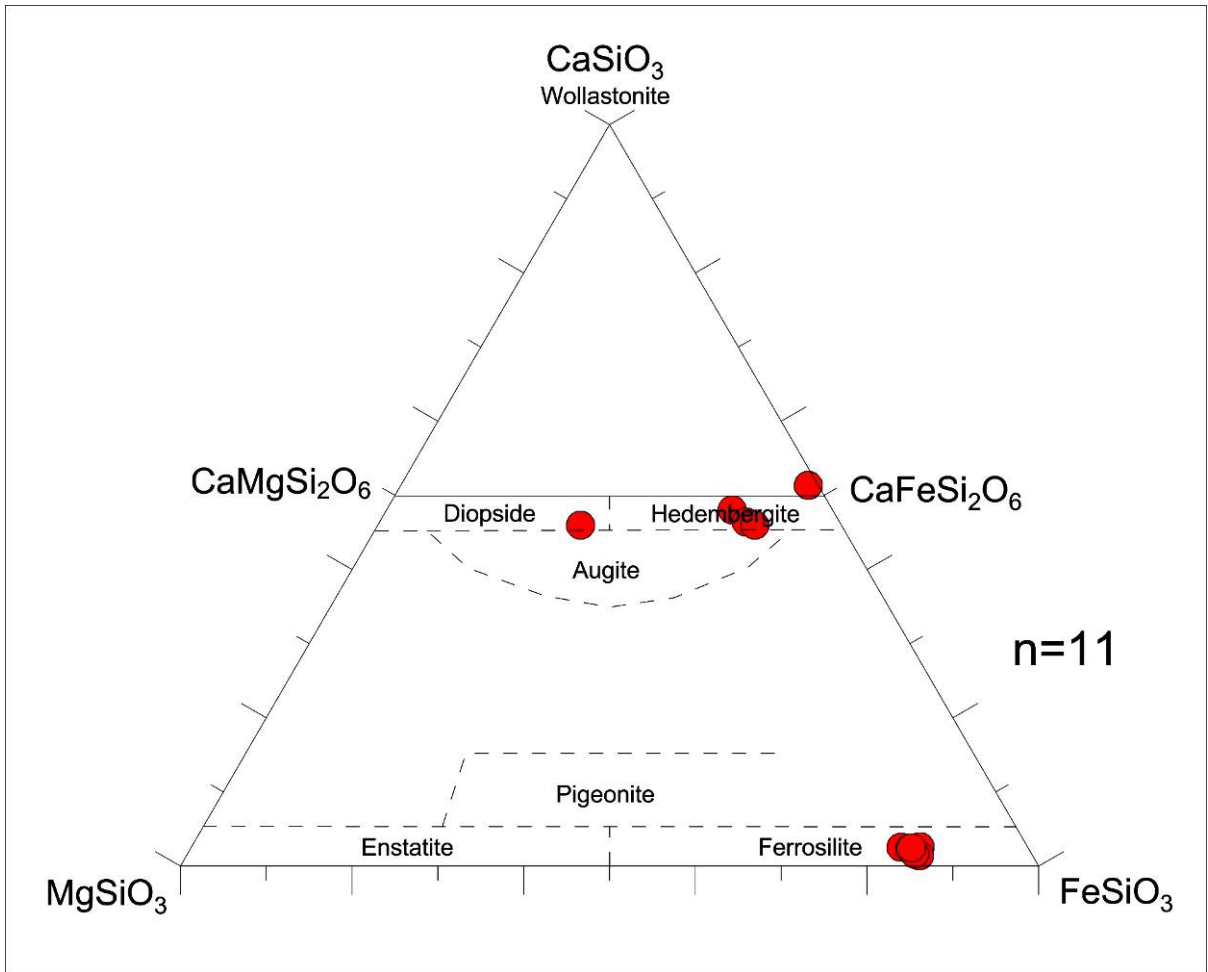


Figure 7: Pyroxene compositions analyzed, plotted in the system  $\text{CaSiO}_3$ - $\text{MgSiO}_3$ - $\text{FeSiO}_3$ .

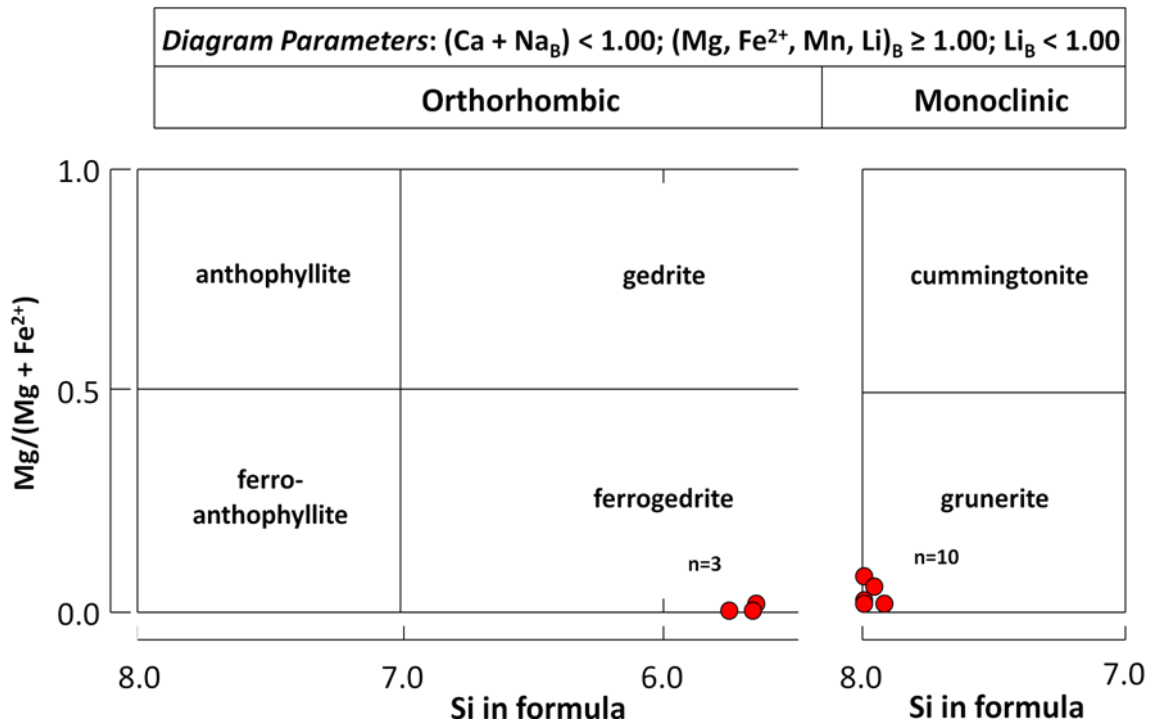


Figure 8: Amphibole analyses plotted, labeled with the nomenclature of Mg-Fe-Mn-Li amphiboles (Leake et al., 1997).

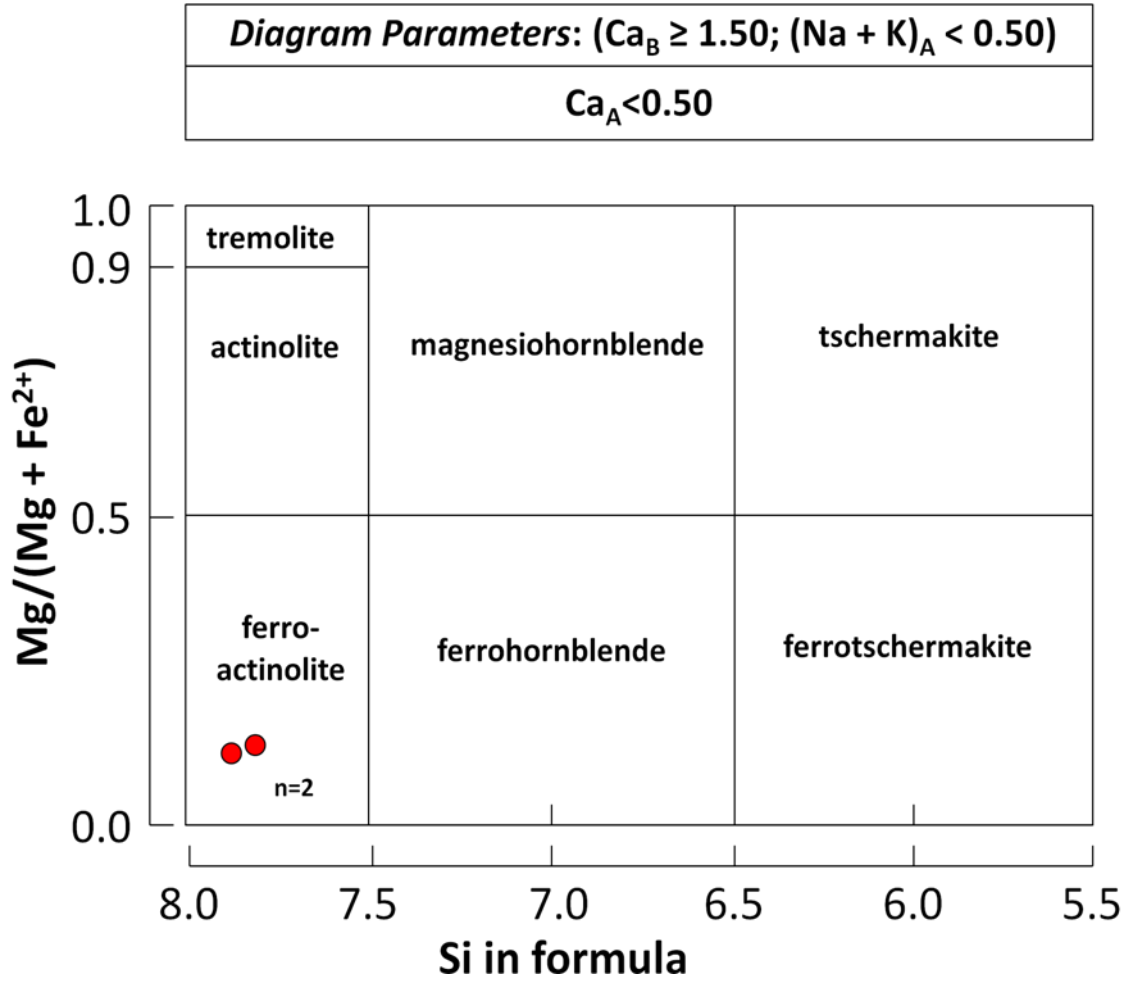


Figure 9: Amphibole analyses plotted, labeled with the nomenclature of calcic amphiboles (Leake et al., 1997).

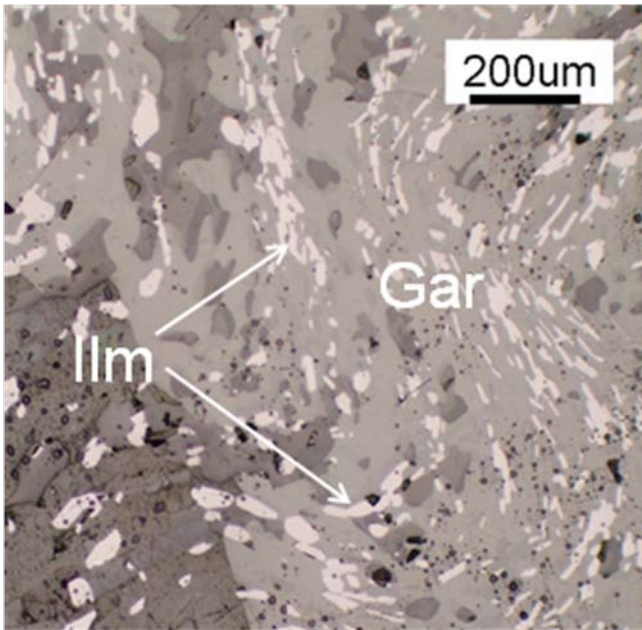


Figure 10: Bedding-parallel Ilmenite grains (Ilm, light gray) as inclusions in a post-metamorphic garnet (Gar, medium gray). Ridge Lake. Photomicrograph, reflective plane polarized light.

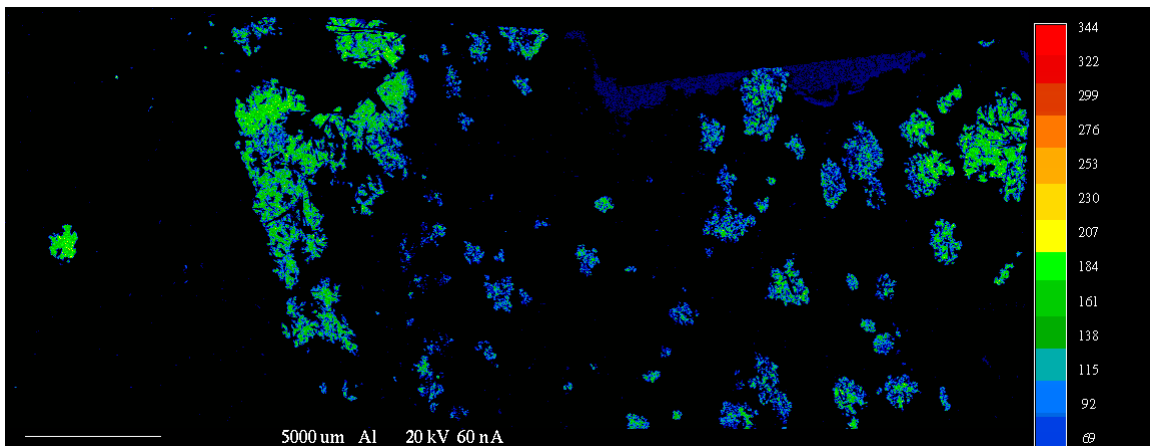


Figure 11: X-ray map for aluminum in a whole this section. All aluminum corresponds to garnets.

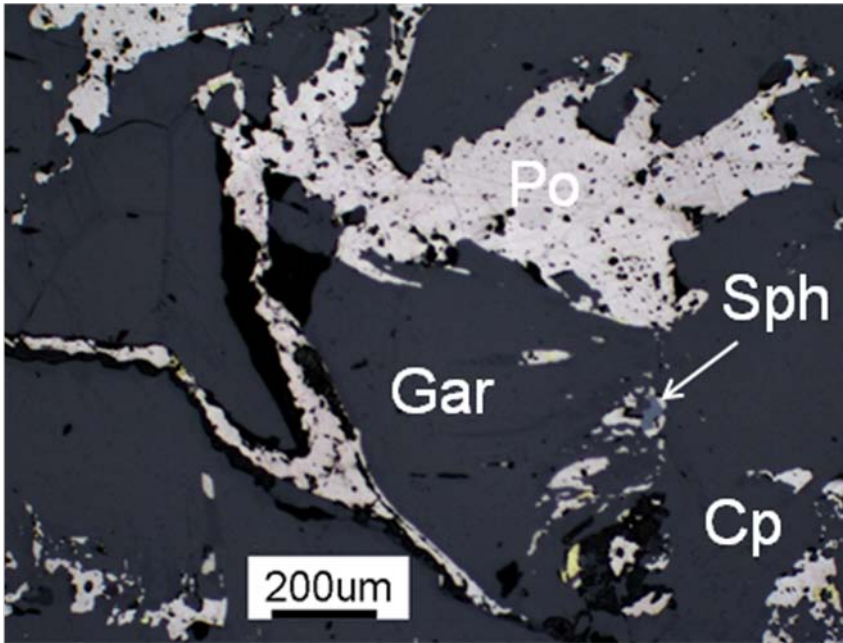


Figure 12: Pyrrhotite (Po), chalcopyrite (Cp), and sphalerite (Sph) mineralization filling interstices, and fractures of, garnet (Gar, dark gray). Ridge Lake. Photomicrograph, reflective plane polarized light.

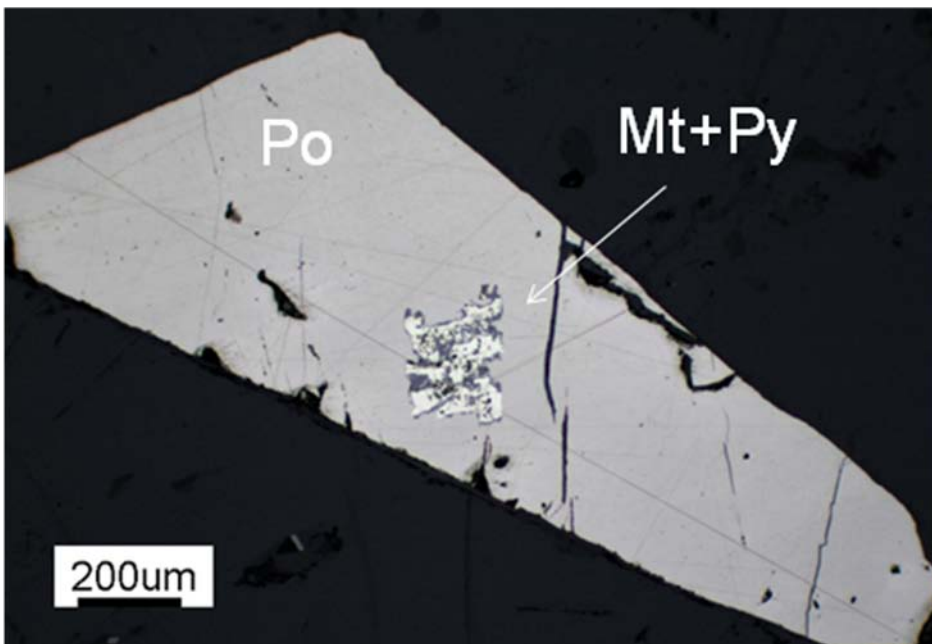


Figure 13: Relicts of pyrite (Py) and magnetite (Mt, gray and white core) replaced by pyrrhotite (Po) grain (creamy white). Malrok. Photomicrograph, reflective plane polarized light.

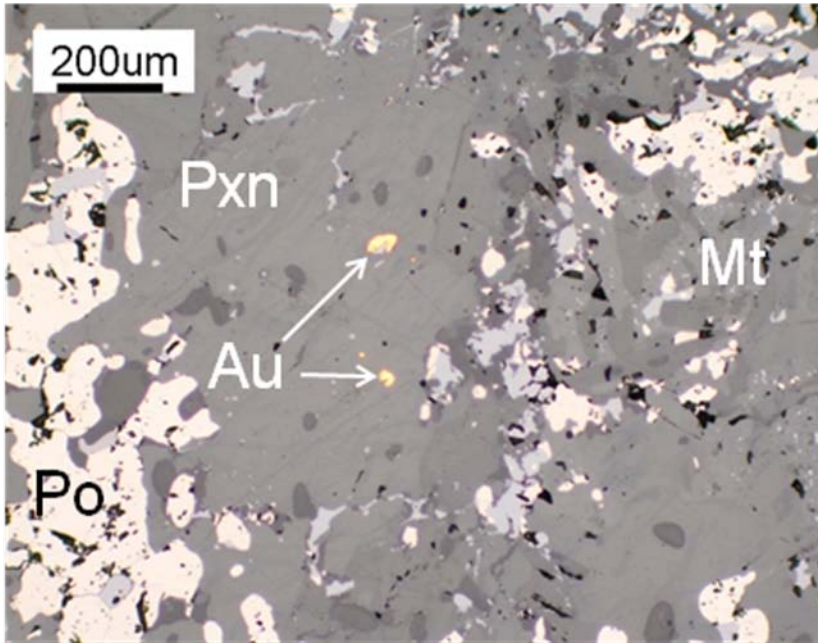


Figure 14: Gold (Au, bright yellow) within clinopyroxene grain (Cpxn) and pyrrhotite (Po) replacing magnetite (Mt). Malrok. Photomicrograph, reflective plane polarized light.

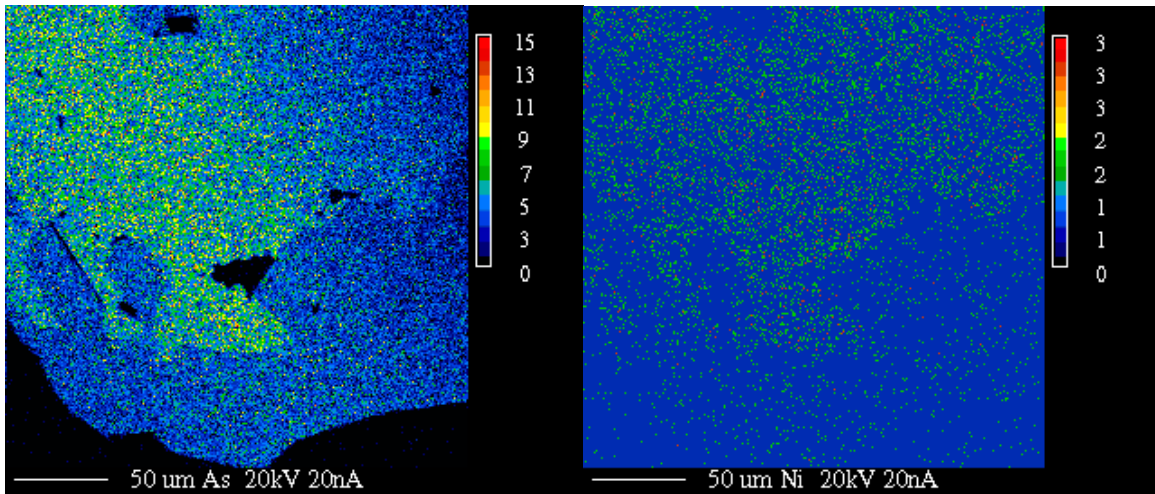


Figure 15: Two x-ray maps for arsenic (left) and nickel (right) in an arsenopyrite grain with a core of loellingite. Note the correspondence between high arsenic and nickel contents in loellingite.

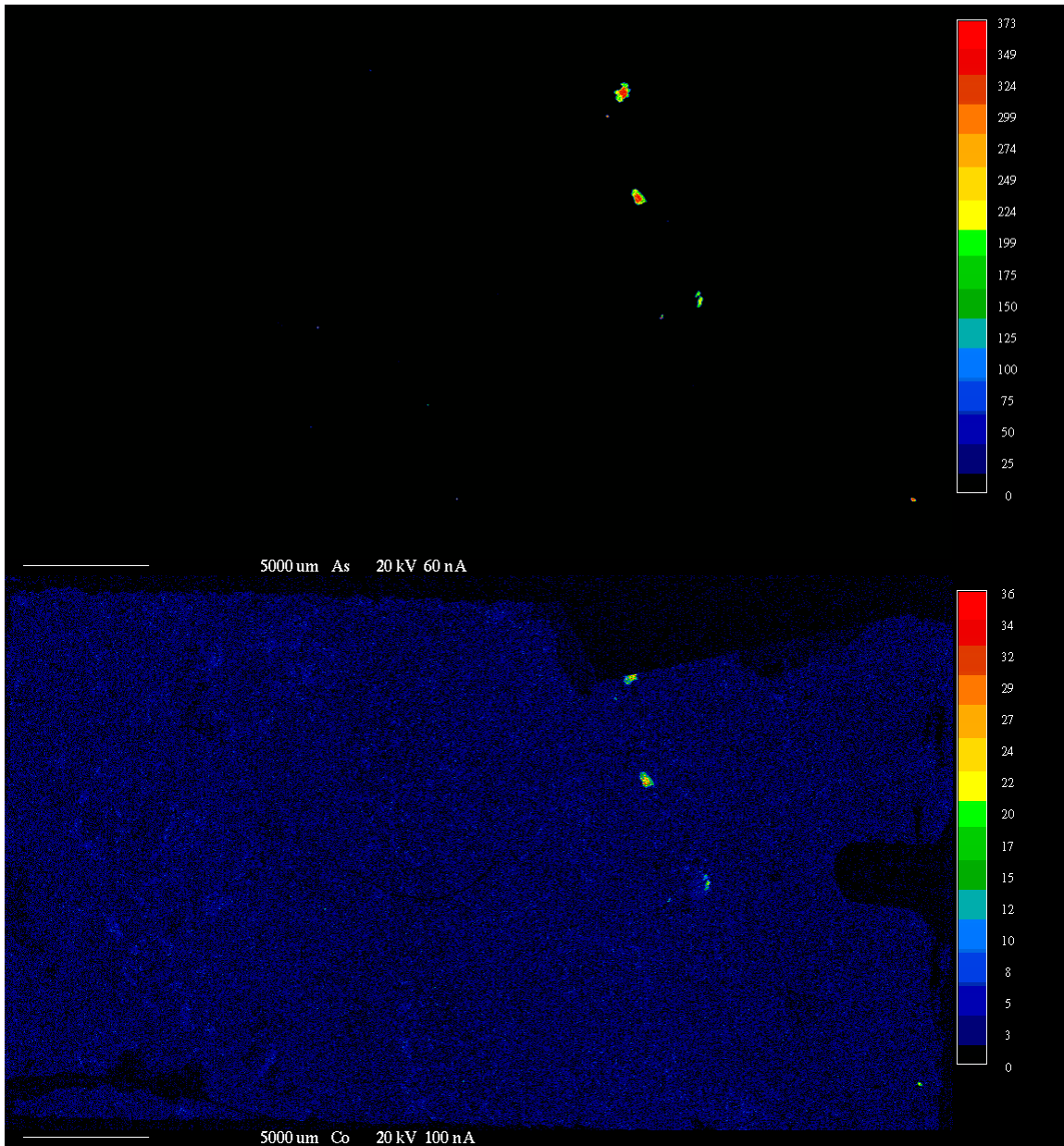


Figure 16: Two x-ray maps for arsenic (up) and cobalt (down) in a whole thin section. Note the correspondence between high arsenic and cobalt contents in arsenopyrite and loellingite (brighter spots).

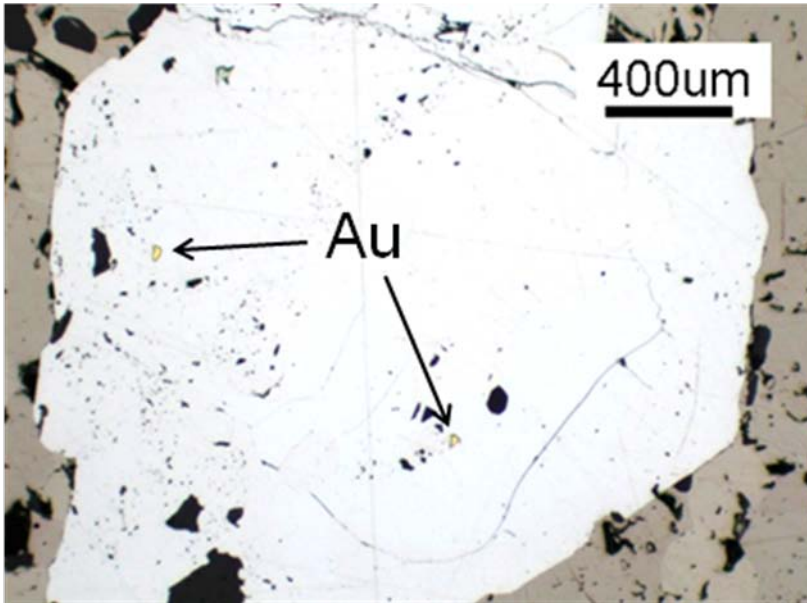


Figure 17: Loellingite (Loe) relicts within euhedral arsenopyrite (Asp); these minerals have very similar optical characteristics; gold (Au) inclusions. The same area as figure 16. Ridge Lake. Photomicrograph, reflective plane polarized light.

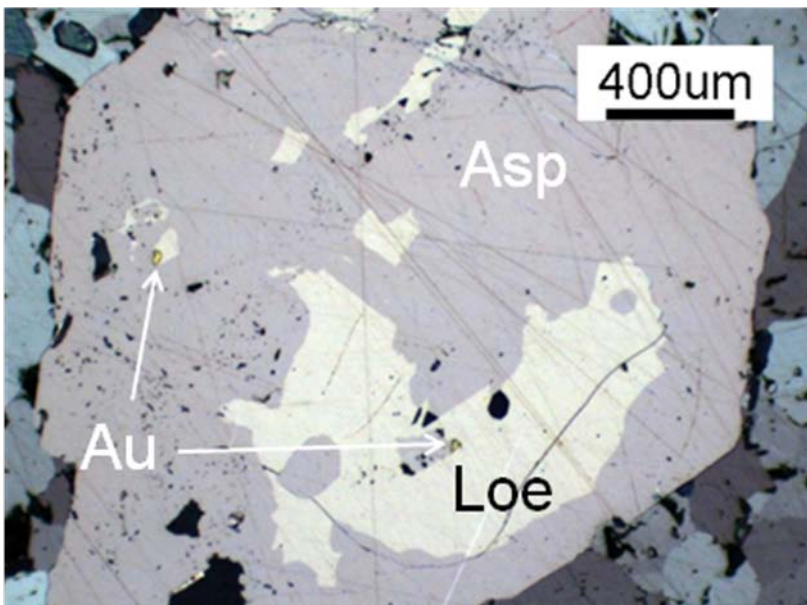


Figure 18: Sometimes loellingite (Loe, white) can be distinguished from arsenopyrite (Asp, light gray) using partially crossed polars, Au (bright yellow) inclusions in border grains of Lo. The same area as Figure 15. Ridge Lake. Photomicrograph, reflective partially crossed polarized light.

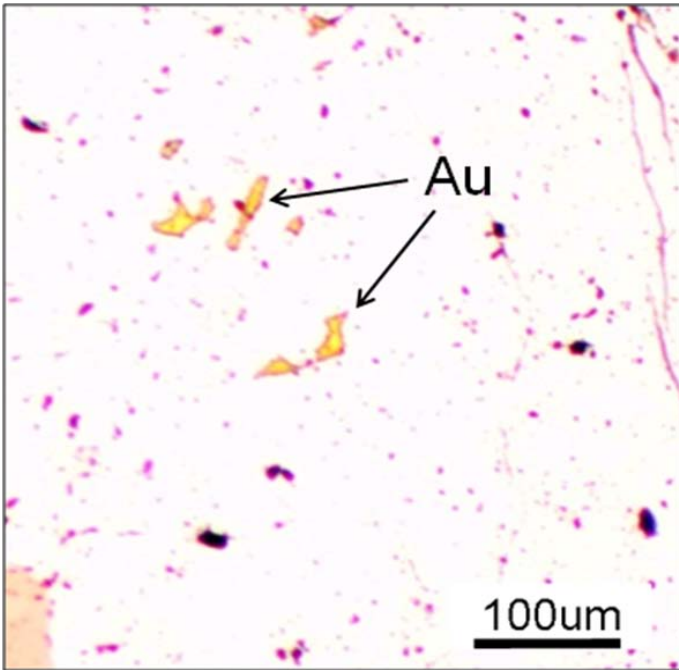


Figure 19: Undistinguished loellingite (Loe) and arsenopyrite (Asp) with several gold (Au, bright yellow) inclusions. The same area as Figure 18. Ridge Lake. Photomicrograph, reflective plane polarized light.

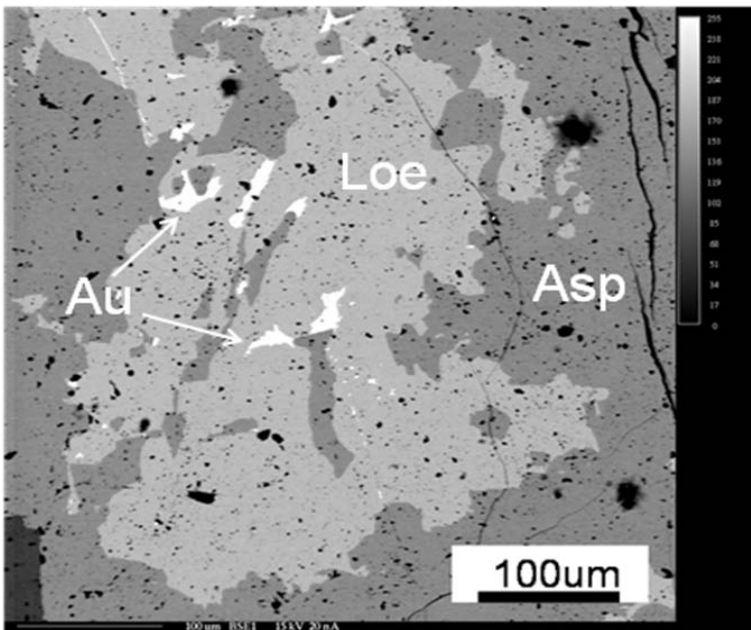


Figure 20: Loellingite (Loe, light gray) relict containing several gold (Au, all white spots) inclusions surrounded by euhedral arsenopyrite (Asp, medium gray); note that gold grains are commonly in contact with both loellingite and arsenopyrite. The same area as Figure 17. Ridge Lake. Photomicrograph, microprobe backscattered image.

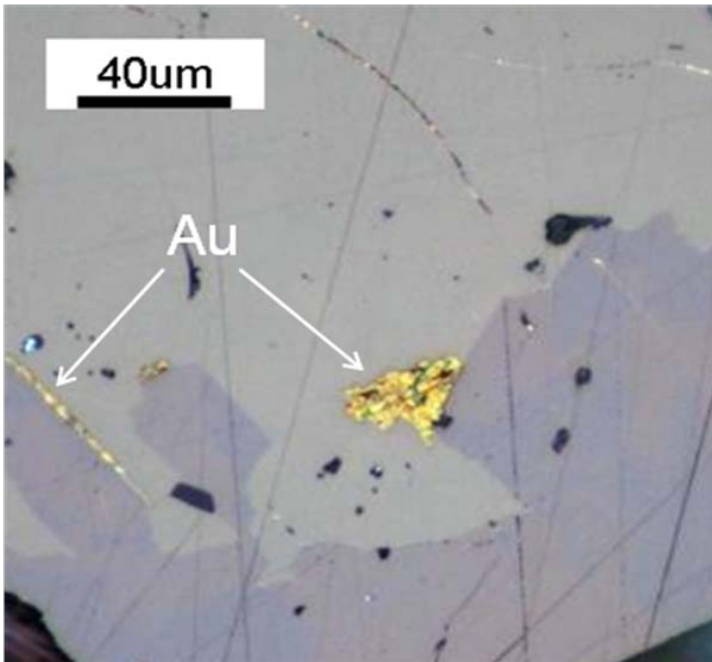


Figure 21: Loellingite relict (Loe, light gray) with gold (Au, yellow) inclusions within arsenopyrite (Asp). The same area as Figure 20. Malrok. Photomicrograph, reflective partially crossed polarized light.

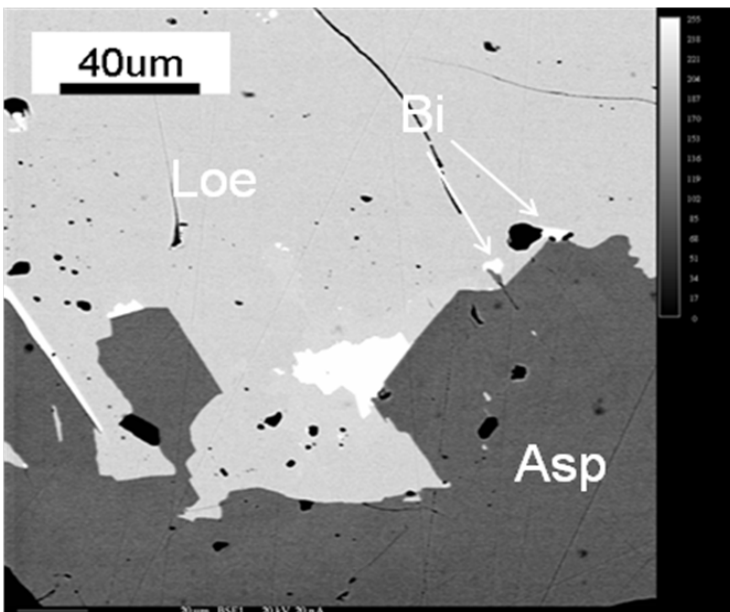


Figure 22: Loellingite relict (Lo, light gray) with gold (Au, some white) and Bi (white spots that are black in Fig. 19) inclusions within arsenopyrite (Asp, dark gray). The same area as Figure 19. Ridge Lake. Photomicrograph, microprobe backscattered image.

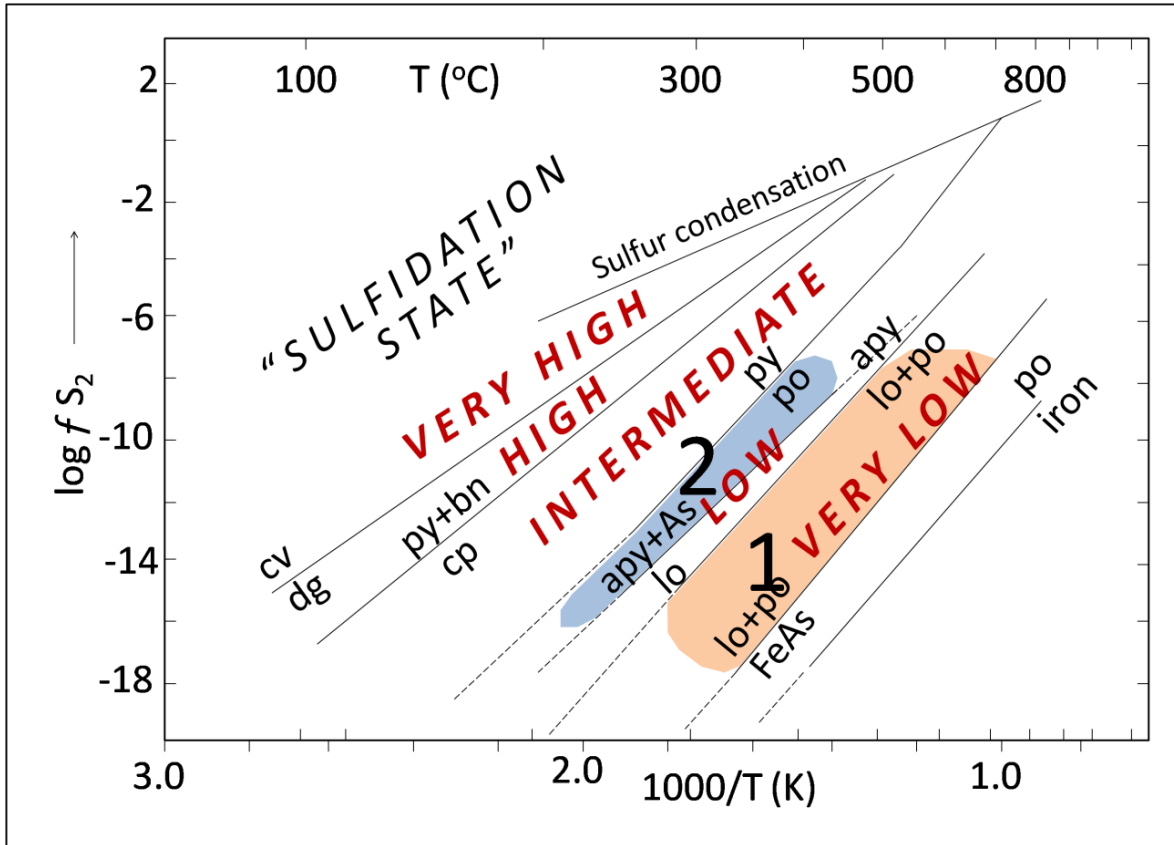


Figure 23: Log  $f_{S_2}$  – 1000/T diagram for various sulfidation reactions, defining the relative sulfidation state for the two mineralization events. Zone 1 constrains conditions for gold, loellingite, and bismuth; and zone 2 pyrrhotite, arsenopyrite and chalcopyrite. Abbreviations: cv: covellite; dg: digenite; py: pyrite; bn: bornite; cp: chalcopyrite; apy: arsenopyrite; po: pyrrhotite; lo: loellingite; As: arsenic; Fe: iron. After Barton and Skinner (1979) and Einaudi et al., (2003).

## Tables

### Table 1

Representative electron microprobe analyses of amphiboles from Marlok and Ridge Lake<sup>1</sup>.

	Malrok 5			Malrok 6		Malrok 10				Malrok 12	Ridge Lake 27		Ridge Lake 39		
	GRU	GRU	CA-FE-GEDR	GRU	GRU	GRU	GRU	CA-FE-GEDR	CA-FE-GEDR	GRU	FE-ACT	FE-ACT	GRU	GRU	GRU
SiO <sub>2</sub>	52,54	51,55	36,95	50,47	49,68	48,55	49,55	36,62	36,88	49,33	52,65	53,14	50,06	50,19	50,23
TiO <sub>2</sub>	0,03	0,07	0,10	0,05	0,03	0,00	0,02	0,09	0,01	0,05	0,04	0,07	0,00	0,00	0,00
Al <sub>2</sub> O <sub>3</sub>	0,25	0,22	20,80	0,42	0,28	0,17	0,14	20,68	20,03	0,38	1,73	1,31	0,17	0,19	0,21
Cr <sub>2</sub> O <sub>3</sub>	0,03	0,00	0,03	0,00	0,01	0,01	0,04	0,02	0,04	0,00	0,00	0,00	0,00	0,00	0,00
Fe <sub>2</sub> O <sub>3</sub>	0,00	0,96	7,97	0,52	1,06	0,88	0,00	7,67	6,89	1,29	0,57	0,19	0,31	1,93	2,22
FeO	27,44	29,20	14,59	37,01	36,22	38,59	38,61	15,91	15,98	37,65	16,46	17,62	38,10	36,06	35,66
MgO	12,42	10,45	1,23	6,28	4,87	4,34	5,09	0,26	0,31	4,74	11,84	12,02	5,99	5,89	5,95
MnO	3,45	3,70	14,05	2,61	3,83	3,79	3,23	12,00	12,41	3,50	2,07	0,84	2,29	2,34	2,27
CaO	1,06	1,01	4,27	0,14	0,77	0,35	0,45	5,96	5,72	0,61	11,67	11,94	0,41	0,43	0,42
Na <sub>2</sub> O	0,05	0,05	0,00	0,08	0,07	0,03	0,01	0,02	0,00	0,06	0,08	0,08	0,00	0,03	0,01
K <sub>2</sub> O	0,01	0,01	0,01	0,01	0,00	0,02	0,01	0,00	0,00	0,00	0,03	0,03	0,00	0,00	0,00
H <sub>2</sub> O	1,97	1,94	1,96	1,89	1,86	1,84	1,86	1,94	1,92	1,87	2,02	2,02	1,88	1,88	1,88
Total	99,26	99,18	101,95	99,48	98,70	98,57	98,99	101,15	100,20	99,49	99,15	99,27	99,19	98,93	98,86
Si	8,00	7,96	5,65	8,00	8,00	7,93	8,00	5,66	5,75	7,93	7,82	7,88	8,00	8,00	8,00
B	0,00	0,00	0,00	0,00	0,00	0,00	0,00	0,00	0,00	0,00	0,00	0,00	0,00	0,00	0,00
Al	0,00	0,04	2,35	0,00	0,00	0,03	0,00	2,34	2,25	0,07	0,18	0,12	0,00	0,00	0,00
Sum	8,00	8,00	8,00	8,00	8,00	7,96	8,00	8,00	8,00	8,00	8,00	8,00	8,00	8,00	8,00
Al	0,04	0,00	1,40	0,08	0,05	0,00	0,03	1,42	1,43	0,00	0,12	0,11	0,03	0,04	0,04
Mg	2,82	2,40	0,28	1,48	1,17	1,06	1,22	0,06	0,07	1,14	2,62	2,66	1,43	1,40	1,41
Fe <sup>2+</sup>	1,69	1,99	0,57	3,02	3,12	3,31	3,30	1,04	1,04	3,23	1,93	2,10	3,20	3,02	2,98
Fe <sup>3+</sup>	0,00	0,11	0,92	0,06	0,13	0,11	0,00	0,89	0,81	0,16	0,06	0,02	0,04	0,23	0,27
Mn	0,44	0,48	1,82	0,35	0,52	0,53	0,44	1,57	1,64	0,48	0,26	0,11	0,31	0,32	0,31
Ti	0,00	0,01	0,01	0,01	0,00	0,00	0,00	0,01	0,00	0,01	0,00	0,01	0,00	0,00	0,00
Sum	5,00	5,00	5,00	5,00	5,00	5,00	5,00	5,00	5,00	5,00	5,00	5,00	5,00	5,00	5,00
Fe	1,81	1,78	1,30	1,89	1,76	1,96	1,91	1,01	1,04	1,84	0,12	0,08	1,90	1,79	1,77
Ca	0,17	0,17	0,70	0,02	0,13	0,06	0,08	0,99	0,96	0,11	1,86	1,90	0,07	0,07	0,07
Na	0,02	0,02	0,00	0,02	0,02	0,00	0,00	0,00	0,00	0,02	0,02	0,02	0,00	0,01	0,00
Sum	2,00	1,96	2,00	1,94	1,91	2,03	1,99	2,00	2,00	1,96	2,00	2,00	1,97	1,87	1,85
Na	0,00	0,00	0,00	0,00	0,00	0,01	0,00	0,00	0,00	0,00	0,00	0,00	0,00	0,00	0,00
K	0,00	0,00	0,00	0,00	0,00	0,00	0,00	0,00	0,00	0,00	0,01	0,01	0,00	0,00	0,00
[]	1,00	1,00	1,00	1,00	1,00	0,99	1,00	1,00	1,00	1,00	0,99	0,99	1,00	1,00	1,00
Sum	1,00	1,00	1,00	1,00	1,00	1,00	1,00	1,00	1,00	1,00	1,00	1,00	1,00	1,00	1,00
Total	16,00	15,96	16,00	15,94	15,91	15,99	15,99	16,00	16,00	15,96	16,00	16,00	15,97	15,87	15,85

<sup>1</sup> Gru: grunerite; Ca-Fe-Gedr: calcian ferro-gedrite; Fe-Act: ferro-actinolite. Data reduction procedure of Schumacher (1997).

Table 2

Representative electron microprobe analyses of pyroxenes from Marlok and Ridge Lake<sup>2</sup>.

	Malrok 5	Malrok 6			Malrok 10				Malrok 12	
	CPX	CPX	CPX	OPX	CPX	CPX	OPX	OPX	OPX	OPX
SiO <sub>2</sub>	51,43	46,68	49,18	47,11	48,59	48,77	46,26	46,24	46,56	46,73
TiO <sub>2</sub>	0,04	0,03	0,03	0,00	0,03	0,04	0,03	0,08	0,07	0,06
Al <sub>2</sub> O <sub>3</sub>	0,17	0,15	0,13	0,11	0,20	0,24	0,11	0,12	0,13	0,09
Cr <sub>2</sub> O <sub>3</sub>	0,02	0,00	0,00	0,00	0,00	0,00	0,00	0,00	0,00	0,00
Fe <sub>2</sub> O <sub>3</sub>	0,36	2,88	0,21	0,00	0,14	0,00	0,03	0,00	0,00	0,00
FeO	14,00	21,26	23,60	40,18	24,16	23,76	42,04	41,69	42,41	41,12
MgO	10,07	3,45	3,37	4,03	3,10	0,33	3,48	3,78	3,68	3,73
MnO	2,26	2,58	3,09	6,16	2,51	2,51	5,71	5,46	5,41	5,97
CaO	21,18	19,77	19,97	0,97	19,70	20,06	1,00	0,95	0,54	0,61
Na <sub>2</sub> O	0,03	0,11	0,11	0,04	0,14	0,15	0,00	0,00	0,03	0,02
K <sub>2</sub> O	0,00	0,00	0,01	0,00	0,00	0,00	0,01	0,01	0,00	0,00
Total	99,56	96,92	99,70	98,59	98,59	95,87	98,66	98,33	98,83	98,33
Si	1,99	1,95	2,00	2,02	2,00	2,09	2,00	2,00	2,00	2,02
Al	0,00	0,00	0,00	0,00	0,00	0,00	0,00	0,00	0,00	0,00
Sum	1,99	1,95	2,00	2,02	2,00	2,09	2,00	2,00	2,00	2,02
Al	0,01	0,01	0,01	0,01	0,01	0,01	0,00	0,00	0,01	0,00
Fe <sup>2+</sup>	0,45	0,74	0,80	1,44	0,83	0,85	1,52	1,51	1,53	1,49
Fe <sup>3+</sup>	0,01	0,09	0,01	0,00	0,00	0,00	0,00	0,00	0,00	0,00
Na	0,00	0,01	0,01	0,00	0,01	0,01	0,00	0,00	0,00	0,00
Ca	0,88	0,89	0,87	0,04	0,87	0,92	0,05	0,04	0,02	0,03
Mg	0,58	0,22	0,20	0,26	0,19	0,02	0,22	0,24	0,24	0,24
Ti	0,00	0,00	0,00	0,00	0,00	0,00	0,00	0,00	0,00	0,00
Mn	0,07	0,09	0,11	0,22	0,09	0,09	0,21	0,20	0,20	0,22
Sum	2,01	2,05	2,00	1,98	2,00	1,91	2,00	2,00	2,00	1,98
Total	4,00	4,00	4,00	4,00	4,00	4,00	4,00	4,00	4,00	4,00

<sup>2</sup> Cpx: clinopyroxene; Opx: orthopyroxene.

Table 3

Representative electron microprobe analyses of garnets from Marlok and Ridge Lake<sup>3</sup>.

	Melrok 10	Ridge Lake 20		Ridge Lake 39	Ridge Lake 41	Ridge Lake 47	
	Alm	Alm	Alm	Alm	Alm	Alm	
SiO <sub>2</sub>	36,15	36,77	37,14	36,87	36,71	36,87	36,75
TiO <sub>2</sub>	0,06	0,02	0,05	0,04	0,05	0,64	0,13
Al <sub>2</sub> O <sub>3</sub>	20,58	21,32	21,73	21,79	20,84	21,15	21,18
Cr <sub>2</sub> O <sub>3</sub>	0,00	0,06	0,10	0,04	0,00	0,16	0,07
Fe <sub>2</sub> O <sub>3</sub>	0,31	0,00	0,00	0,00	0,00	0,00	0,00
FeO	25,24	31,35	33,36	33,10	27,60	30,02	30,72
MgO	0,38	1,86	2,27	2,68	0,45	1,16	0,85
MnO	12,45	5,71	4,09	4,17	9,01	6,76	5,29
CaO	3,66	2,50	1,84	1,56	4,83	3,65	4,81
Na <sub>2</sub> O	0,01	0,02	0,02	0,00	0,00	0,04	0,01
K <sub>2</sub> O	0,00	0,00	0,01	0,00	0,00	0,01	0,00
Total	98,85	99,62	100,61	100,24	99,49	100,46	99,83
Si	5,97	5,97	5,96	5,93	6,00	5,96	5,97
Al	0,00	0,00	0,00	0,00	0,00	0,00	0,00
Sum	5,97	5,97	5,96	5,93	6,00	5,96	5,97
Al	4,01	4,08	4,11	4,13	4,02	4,03	4,06
Fe <sup>3+</sup>	0,04	0,00	0,00	0,00	0,00	0,00	0,00
Ti	0,01	0,00	0,01	0,00	0,01	0,08	0,02
Sum	4,05	4,08	4,12	4,13	4,02	4,11	4,07
Fe <sup>2+</sup>	3,49	4,26	4,48	4,45	3,77	4,06	4,17
Ca	0,65	0,44	0,32	0,27	0,85	0,63	0,84
Mg	0,09	0,45	0,54	0,64	0,11	0,28	0,20
Cr	0,00	0,01	0,01	0,00	0,00	0,02	0,01
Mn	1,74	0,79	0,56	0,57	1,25	0,93	0,73
Sum	5,97	5,94	5,91	5,94	5,98	5,92	5,95
Total	16,00	15,99	15,99	16,00	16,00	15,99	16,00

<sup>3</sup> Alm: almandine.

Table 4

Mineralogical characteristics and associations of gold in samples from Malrok and Ridge Lake projects.

<b>Gold occurrence and mineral association</b>			
<b>Mineral</b>	<b>%</b>		<b>Number of grains</b>
Amphibole	1.0		587
Amphibole altering clinopyroxene	3.9		
Clinopyroxene	3.1		
Orthopyroxene	0.2		
Garnet	1.0		
Amphibole altering garnet	0.2		
retrograde aggregate	1.7		
Quartz	7.2		
Loellingite	66.6		
Arsenopyrite	15.0		
Bismuth	0.2		
		<b>Maximum size (µm)</b>	95
		<b>Minimum size (µm)</b>	1
		<b>Average</b>	9.4
		<b>Free gold (%)</b>	18.2
		<b>Gold as inclusion in other metals (%)</b>	81.8
		<b>Gold in border between loellingite and arsenopyrite (%)</b>	31.0
		<b>Gold grains in Malrok (%)</b>	10.7
		<b>Gold grains in Ridge Lake (%)</b>	89.3

Table 5

Summary of characteristic features of selected gold-bearing BIF deposits<sup>4</sup>.

Name	Location	Age	Deformational Events	BIF Facies	Metamorphic Facies	Structural Control	Alteration	Replacement	Gold Occurrence	Gold:Silver Ratio	Reserves and Gold Content	Reference	Reference
<b>Baffin Island</b>	Baffin Island - Canada	Paleo-Proterozoic	3	Silicate-Sulfide	Amphibolite to Granulite	Unknown	Not identified	Mt, Py, and Ilm replacement by Po	Loe-Asp boundaries - Contact with sulfides - Free with silicates	4.2 - 44.1	-	The present work	
<b>Homestake</b>	Lead, South Dakota - USA	Paleo-Proterozoic	2	Carbonate-Sulfide	Green Schist to Lower Amphibolite	Hinges of folds	Chl-Sid-Ser	Gold-rich vein selvage	Contact and fractures of Asp - Associated with Po	6.2	40 Moz - 150 Mton	Caddey et al., 1991	Nelson, 1985
<b>Agnico-Eagle</b>	Quebec - Canada	Archean	1	Carbonate-Silicate-Sulfide	Green Schist + Contact Metamorphism	Fe-dolomite veins - Shear zones	FeDol-Chl-(Asp veins)	None	Within fine euhedral Py	5.0	~0.8 Moz - 4 Mton	Wyman et al., 1986	Kerswill, 1995
<b>Sao Bento</b>	Minas Gerais - Brazil	Archean	3	Oxide (Carbonate-Sulfide)	Green Schist	Thrust faults and shear zones	Sulfidation (Asp-Po)-Ank - (Dol halos)	Mt replacement by Asp and Po	Inclusions in sulfides - edges of sulfides - free	9.0	1.9 Moz (2001+reserves)	Martins et al., 2007	Kerswill, 1995
<b>Lupin</b>	Northwest Territories - Canada	Archean	3	Silicate (Sulfide)	Amphibolite - Lower Granulite	Qz veins	Hb - Sulfidation	Pervasive replacement of Gru by Hb	Inclusions in sulfides - Loe-Asp boundaries	6.0	3.8 Moz - 11.7 Mton	Bullis et al., 1993	
<b>Mt Morgans</b>	Yilgarn Block - Australia	Archean	4	Sulfide-Carbonate	Green Schist	Restricted to shear and fault zones	Qz-Sid veins with Py halo - Sulfidation	Mt by Py	Inclusions in Py - Free and inclu in Cp or Sph	866 (6.3)	0.78 Moz	Vielreicher et al., 1994	
<b>Vubachikwe and others</b>	Gwanda Greenstone Belt - Zimbabwe	Archean	2	Carbonate-Sulfide	Green Schist	Discordant vein type mineralization	Retrograde Chl	Mt by Rut	Inclusions in Asp (or Po)	~12	~1 Moz altogether	Saager and Oberthuer, 1989	
<b>Cuiaba</b>	Minas Gerais - Brazil	Archean	3	Carbonate	Green Schist	Structurally controlled ore shoots	Sulfidation (Chl-Carb-Ser)	Replacement of Sid-Ank by Fe-sulfides	Inclusions - Fractures - Boundaries in Py	840 (6.0 average)	6.5 Moz only reserves 2007	Ribeiro et al., 2007	Ribeiro et al., 1998
<b>Morro Velho</b>	Minas Gerais - Brazil	Archean	4	Sulfide	Green Schist	Some remobilization into the hinge zone of folds	Unknown	None	Within or along sulfide silicate boundaries	5.0	16 Moz - 50 Mton	Vieira et al., 1991	Kerswill, 1995

<sup>4</sup> Chl: chlorite; Sid: siderite; Ser: sericite; Ank: ankerite; Carb: carbonates; Dol: dolomite; Hb: hornblende; Qz: quartz; Rut: rutile; Py: pyrite; Asp: arsenopyrite; Po: pyrrhotite; Fe: iron.